UNIVERSITÀ DEGLI STUDI DI TRIESTE
e
UNIVERSITÀ CA' FOSCARI DI VENEZIA

XXXI CICLO DEL DOTTORATO DI RICERCA IN CHIMICA

Pin1 protein: a druggable target in high grade serous ovarian cancer

Settore scientifico-disciplinare: **Ingegneria chimica**

DOTTORANDO / A
CONCETTA RUSSO SPENA

COORDINATORE
PROF. BARBARA MILANI

SUPERVISORE DI TESI
PROF. MARIO GRASSI

CO-SUPERVISORE DI TESI
PROF. FLAVIO RIZZOLIO

ANNO ACCADEMICO 2017/2018

Abstract

The prolyl isomerase Pin1 is overexpressed in different types of cancer and sustains the tumor progression. The inactivation of Pin1 restrains the tumor progression. In my PhD I showed that in high-grade serous ovarian cancer Pin1 is an important therapeutic target and the knock down of Pin1 restrains the tumor growth in a syngeneic mouse model. Also, I designed the fist liposomal formulation of Pin1 since no Pin1 inhibitor are able to down regulate the function of this protein in vitro but also in vivo. The inhibitor was encapsulated in modified cyclodextrins and then via a pH gradient was loaded inside pegylated liposomes. The liposomal formulation accumulates in the tumor reducing the tumor volume and had a desirable pharmacokinetic profile. Nevertheless, the liposomal inhibitor was able to alter Pin1 cancer driuving-pathways trough the induction of proteasome-dependent degradation of Pin1.

1. Introduction

1.1 High grade serous epithelial ovarian cancer (HGS-EOC)

Epithelial ovarian cancer (EOC) is the leading cause of death in gynecological cancer in developed countries and the fifth most common cause of cancer mortality in women: 80% of deaths are patients presenting high-grade serous ovarian cancer with advanced-stage [1]. Most ovarian cancer patients (60%) are diagnosed with distant-stage disease, for which 5-year survival is 29%. As a result, the overall 5-year relative survival rate for ovarian cancer is low (47%).

Approximately 15% of ovarian cancers are familial and 85% sporadic. Conventionally, ovarian cancers have been thought to develop from ovarian surface epithelial cells into cancers that resemble epithelium of the endometrium, Fallopian tube, mucin secreting endocervical glands and glycogen-filled vaginal rests. A distinctive feature of ovarian cancer is the ability to spread through the abdominal cavity, forming nodules on the surface of the parietal and visceral peritoneum including the omentum [2]. The epithelial ovarian cancer in fact can spread through lymphatic and blood vessels to nodes and parenchyma of distant organs, including the liver.

At a molecular, cellular and clinical level, ovarian cancers can be divided into two different groups based on histological grade and molecular genotype and phenotype. The **type I** cancers are mucinous, endometrioid, low grade of serous, or clear-cell histotype. They are frequently diagnosed in an early stage, and resist chemotherapy but could respond to hormonal manipulation. Type I have wild-type p53 and BRCA1/2, with frequent mutation in Ras, Raf and KRAS genes. The more prevalent **type II** cancers are endometrioid, high grade of serous or undifferentiated histotypes. These cancers grow aggressively, are defined only in a late stage (III–IV) and respond to conventional chemotherapy but less often to hormonal manipulation (Fig.1)[2].

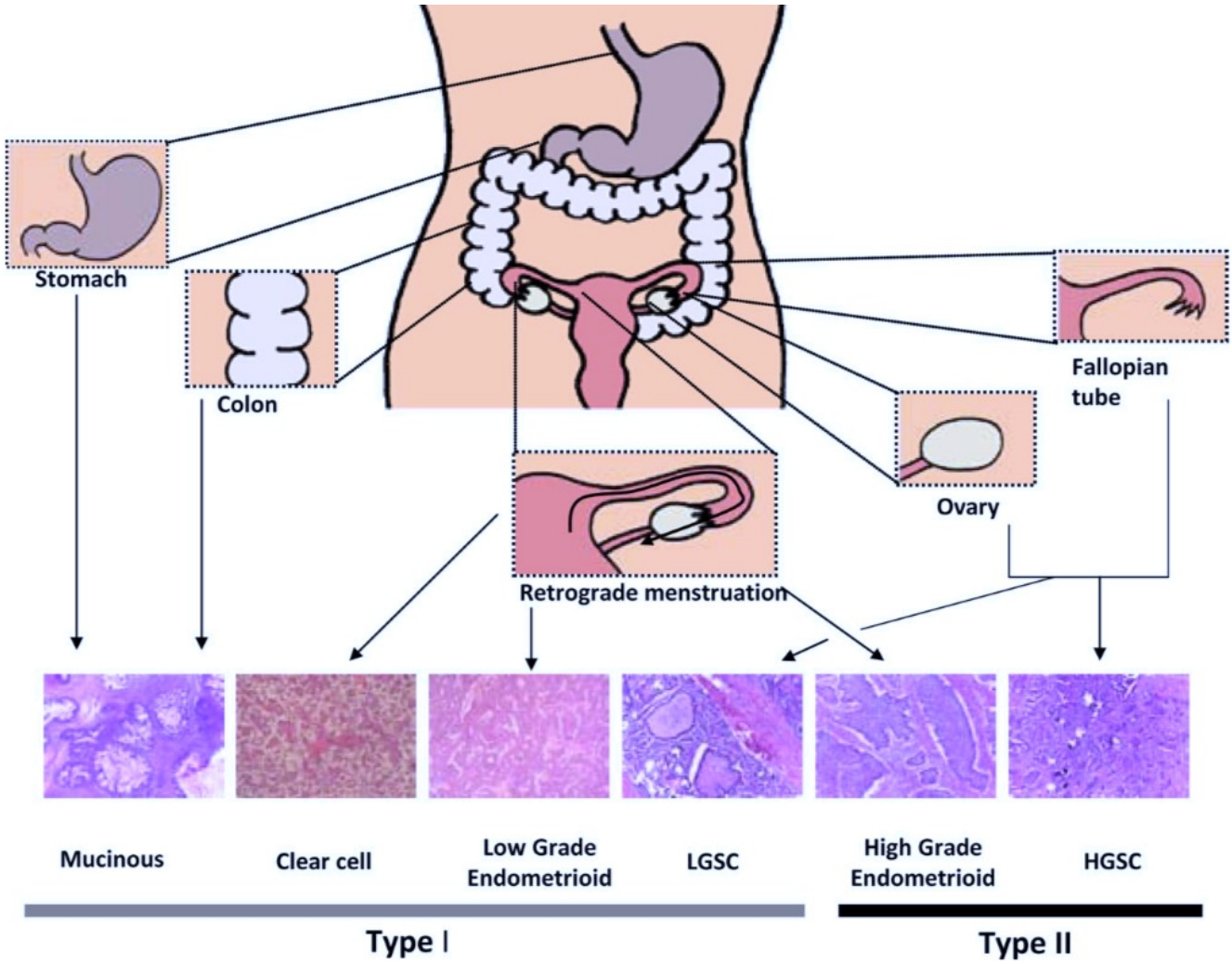

Fig.1 Origin and histological subtypes associated with type I and type II [2].

Different studies are focused on the definition of the origin and the treatment of the most aggressive type of ovarian cancer: the high-grade serous epithelial ovarian cancer (HGS-EOC).

Recent findings indicate that many ovarian cancers are derived from non-ovarian tissue: in particular the origin of high-grade serous ovarian cancer is still debated and discussed. More recently the distal fallopian tube has been identified as a source of high-grade ovarian cancers but also the surface of ovary can contribute to the origin of this disease: the relative contribution to the epithelial ovarian cancer remains unclear [3]. A recent study conducted in the mouse model, showed a predominant and principal role of the fallopian tube as the primary origin of HGS-OEC. In fact, by conditionally deleting DICER and Pten double-knockout mice present primary fallopian tube

tumors spread to engulf the ovary and then aggressively metastasize throughout the abdominal cavity. These fallopian tube tumors highly express genes that are known to be up-regulated in human serous ovarian cancers [4]. The relative importance of the fallopian tube compared with the ovarian surface epithelium in the genesis of high-grade serous ovarian cancers is still being discussed, however, this finding has important implications for screening, prevention and understanding the molecular biology of the disease [3] .

Major risk factors for ovarian cancer comprehend the advancing age and the number of ovulatory cycles and also a positive family history of ovarian, breast, uterine, or colon cancer associated to mutations of *BRCA1*, *BRCA2*, mismatch repair genes, or *TP53* in the germ line. Risk is slashed by the use of oral contraceptives for as long as 5 years before menopause, possibly related to reduced ovulation and treatment of transforming cells with progestational agents.

Stage at diagnosis varies by cancer subtype and the high-serous carcinomas are diagnosed at a distant stage (79%), which reflects the aggressive nature of this subtype [5]. Evidences from different cases shown that the high-grade serous ovarian cancer do not present obvious signs of cancer until advanced disease, so the diagnosis is difficult at the time when a curative approach is still feasible. For this type of cancers, debulking surgery and chemotherapy remain the standard therapy [6]. Both the European and American guidelines recommend surgery as the primary approach to ovarian malignancies [7,8]; among these procedures are the total abdominal hysterectomy, bilateral salpingo-oophorectomy, omentectomy, visualization of all peritoneal surfaces, and random peritoneal biopsies plus peritoneal washing. Excision or biopsying any suspicious peritoneal area and sampling lymph nodes are also recommended practices. The goal of primary surgery is the absence of residual cancer. After surgery, adjuvant chemotherapy is obligatory in cases of suboptimal debulking, advanced stages, or early stages that can have a high risk of recurrence. Platinum agents have been considered the major resource in the medical treatment of EOC and evidence from different clinical trials established the paclitaxel and carboplatin combination regimen as the first-

line chemotherapeutic treatment[9]. The cisplatin and paclitaxel doublet was demonstrated to be more effective than cisplatin and cyclophosphamide [10] [11]. The treatment of EOC is characterized by a high response rate to primary treatment (around 75%), which is rapidly followed by early recurrence. At this point, some patients benefit from second-line treatment with platinum, most of patients became platinum-resistance and die from the disease [12]. Thanks to the data reported in the Cancer Genome Atlas project, the molecular targeted therapy of ovarian cancer given alone or integrated with chemotherapy is showing promising results [1] .

The Cancer Genome Atlas project conducted an extensive genomic and transcriptomic characterization of ovarian high-grade serous carcinoma analysing the messenger RNA expression, microRNA expression, promoter methylation and DNA copy number in 489 adenocarcinomas and the DNA sequences of exons from coding genes in 316 of these tumours. The results of this study shown at molecular level an amplification and overexpression of genes in the PI3K family, germline mutation in BRCA1/2 and p53. The mutation in p53 gene is present in the 96% of cases of high-grade serous cancers analysed [2]. From the TGCA study emerged the relevant role of TP53 mutations, extensive DNA copy alterations in different key proteins, preliminary transcriptional signatures associated with survival, varied mechanisms of BRCA1/2 inactivation, and CCNE1 aberrations [13]. These key finding were summarized and reported as a defect and alteration in 4 different signalling pathways:

- **RB and PI3K/RAS pathways** are commonly altered. Alterations are defined by somatic mutations, DNA copy number changes or, in some cases, by significant up or down regulation relative to expression in diploid tumours. Alteration frequencies are defined as a percentage of all cases; activated genes are red and inactivated genes are blue (Fig.2).

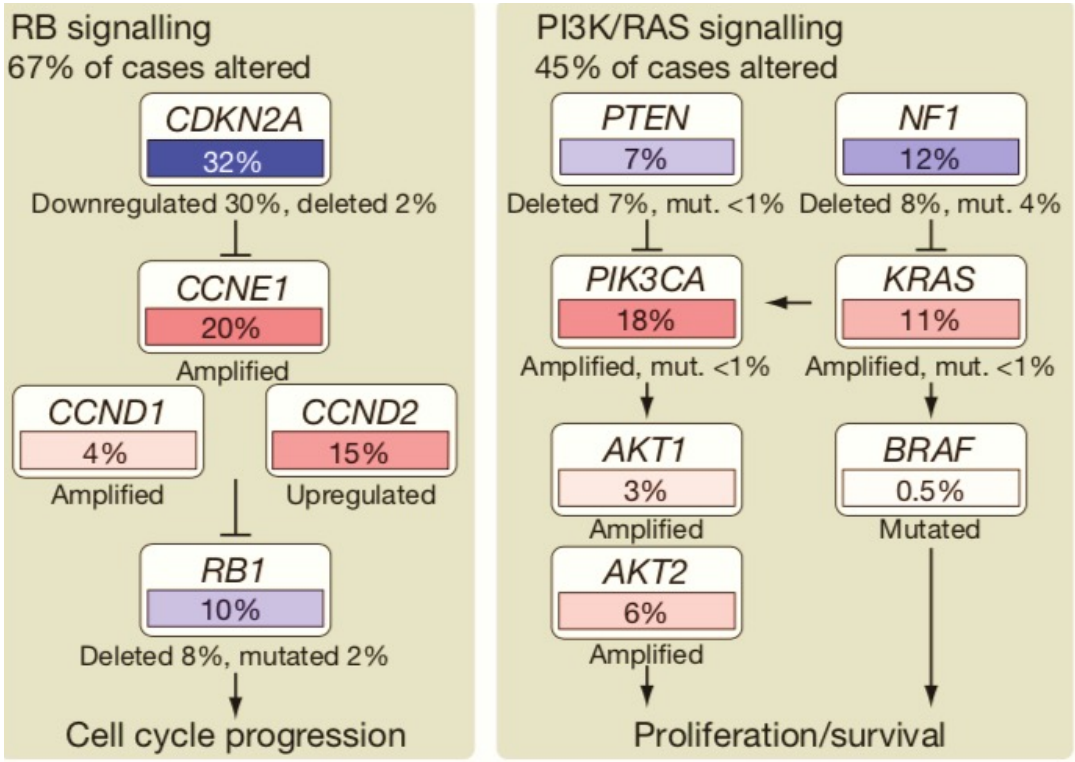

Fig.2 RB and PI3K/RAS signalling altered in HGS-OC [14].

- the **homologous recombination** (HR) pathway is altered in up to 51% of cases.
- the **FOXM1** transcription factor network is activated in 84% of cases.
- the data reported from the Cancer Genome Atlas Research Network described a defect in the **NOTCH signalling** in 22% of cases.

All this altered pathways are involved in the physiology of high-grade serous ovarian cancer [14].

The (HGS)-EOC is the most common and aggressive type of EOC characterized by diagnosis in late stage and resistance after therapeutically treatment. Also, how reported from the TGCA in this type of cancer different pathways are compromised and in the 96% of patients there is a mutation in the p53 protein. Among cofactors that synergize with mutant p53 in the oncogenesis process, Pin1 has been demonstrated to activate a mutant p53 transcriptional program to increase aggressiveness in cancer cells [15].

1.2 Pin1 protein

Numerous oncogenes and tumor suppressors are directly regulated by Pro-directed phosphorylation and/or are part of signalling pathways involving phosphorylation. Notably, the same kinases and phosphatases often act on both oncogenes and tumour suppressors. Indeed, it was not clear until recently how these phosphorylation events are coordinated to promote or inhibit tumorigenesis [16]. Proline uniquely adopts cis and trans conformations, a process that is catalysed by peptidyl-prolyl isomerases (PPIases). Although PPIases can control the interconversion kinetics of *cis*/*trans* isomerization — an intrinsic conformational switch — they were thought to perform non-essential cellular roles, and the significance of this enzymatic activity as an important regulatory mechanism in human physiology and pathology was not known until the discovery of PIN1. PIN1 specifically isomerizes pSer/Thr-Pro motifs, which is especially important because Pro-directed kinases and phosphatases are conformation-specific and act only on the *trans* conformation [17]. Additionally, the phosphorylation severely reduces the already slow rate of isomerization of Ser/Thr-Pro bonds and makes the phosphopeptide bond resistant to the catalytic action of conventional PPIases [18]. Pro-directed phosphorylation also induces local structural changes that make it accessible to further modifications. So, a fundamental mechanism to control key proteins in these pathways is the phosphorylation of the proline (Pro)-Ser/Thr motifs, which are controlled by the **Peptidyl-prolyl cis-trans isomerase NIMA-interacting 1 (Pin1)**, a unique Peptidyl-prolyl isomerases (PPIase) [19] [20].

Structurally, PIN1 is an enzyme with two different domains: WW domain and a catalytic domain with a flexible linker. By binding only to the specific pSer/Thr-Pro motifs, the WW domain targets Pin1 close to its substrate, whereas the PPIase domain catalyses the cis-trans isomerization to regulate the structure and function of its substrate; both domains are required for PIN1 function in vivo. The WW domain (named after two invariant Trp residues) is situated in the N-terminal

whereas the C-terminal presents the PPIase domain (Fig. 3a). Early structure–function analyses *in vitro* and *in vivo* have revealed that the unique substrate specificity of PIN1 towards specific pSer/Thr-Pro motifs results from interactions provided by both of these domains — a 'double-check' mechanism [21] [22,23]. The WW domain always binds only to specific pSer/Thr-Pro-motifs, which are often crucial regulatory phosphorylation sites in PIN1 substrates [24] [25] whereas the PPIase domain isomerizes specific pSer/Thr-Pro motifs to regulate protein function by controlling their conformations (Fig. 3c).

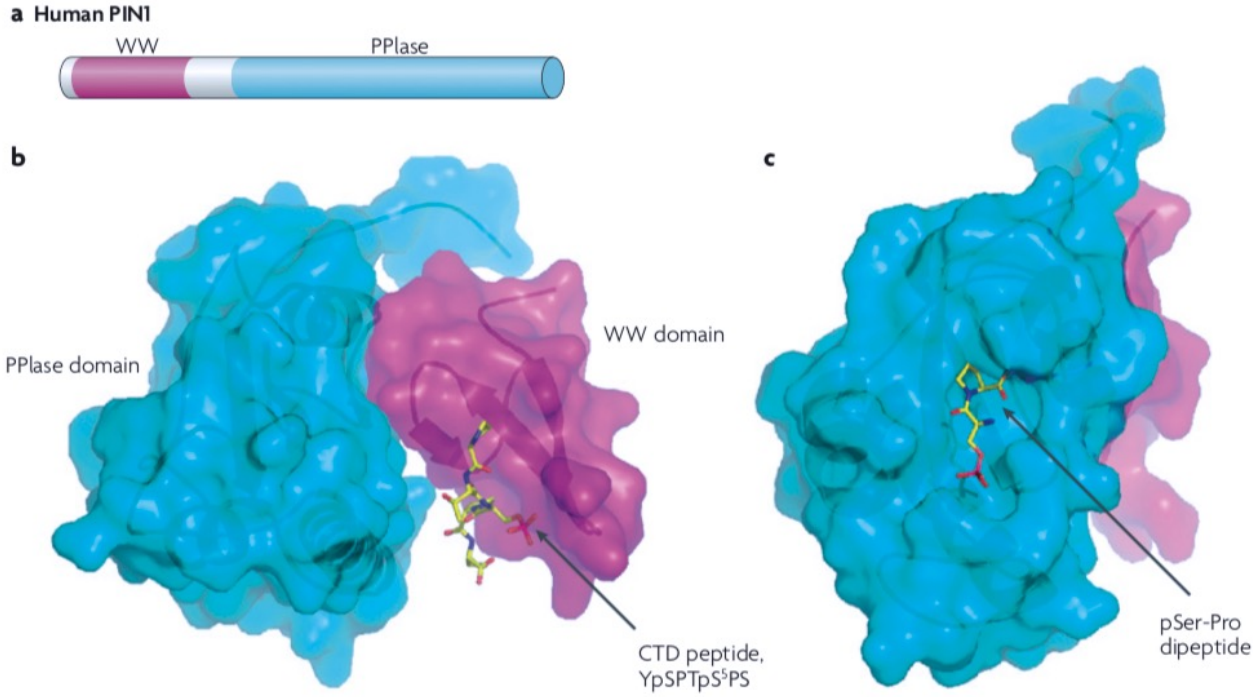

Fig. 3 Structure of PIN1 protein. (A) PIN1 contains an N-terminal WW domain, which mediates binding to specific pSer/Thr-Pro motifs, and a C-terminal peptidyl-prolyl cis/trans isomerase (PPIase) domain that catalyses isomerization of specific pSer/Thr-Pro motifs in the substrate. (B and C) X-ray structures of PIN1 in a complex with a C-terminal domain (CTD) peptide ($YpSPTpS^5PS$) [26].

The structures of PIN1 in complex with its binding phosphopeptides have confirmed the phosphorylation-dependent interaction [27,28]. It remains unclear why PIN1 binds only to specific

pSer/Thr-Pro motifs in certain proteins. The sequence that is crucial for the PIN1-binding specificity is located in the WW domain at an intrinsically flexible loop, the flexibility of which changes upon ligand binding, suggesting that sequence-specific dynamics are important for PIN1 substrate specificity [18]. It is also not fully clear how WW and PPIase domains are coordinated to act on PIN1 substrates.

The subcellular localization and function of PIN1 are dependent on the availability of its substrates: PIN1 can bind its substrates in the different subcellular compartments which must be phosphorylated on specific Ser/Thr-Pro motifs [29]. Many of PIN1's substrates contain a single phosphorylation target in the form of CDC25, WEE1 and RPB1. Others, like CK2 and Sil, have multi-phosphorylation sites, suggesting a different mechanism in PIN1 function.

In cell cycle control, PIN1 was originally identified and defined as a protein important in mitosis. In G1/S progression PIN1 modulates the well-known cell cycle regulators, like cyclin D1, RB, p53, p27, and cyclin E. In particular, PIN1 can increase cyclin D1 gene expression by multiple mechanisms, including activation of the c-Jun/c-Fos, beta-catenin/T-cell transcription factor (TCF) and nuclear factor (NF)-kB transcription factors [24,25,30]. Furthermore, PIN1 can directly bind to phosphorylated cyclin D1 and stabilize its protein stability. Moreover, *Pin1*-knockout mice display a phenotype that resembles cyclin D1-knockout mice in some tissues such as the mammary gland. During G2/M transition, it was shown that Aurora A suppresses Pin1 activity through phosphorylation at Ser16 and cooperates with hBora to modulate G2/M transition.

Depletion of PIN1 in yeast and human cells induces mitotic arrest and its over-expression blocks the cells in the G2 phase of the cell cycle. Depending on cellular context, inhibition of PIN1 affects cellular proliferation, epithelial mesenchymal transition, migration and invasion, new angiogenesis, and apoptosis. It could be conclude that PIN1 may be thought of as a molecular timer that modulates cell cycle progression networks.

Many protein kinases that are activated in response to various stresses are Pro-directed kinases, and PIN1 has been shown to regulate the function of several key proteins that are involved in various cellular stress responses. How reported previously, many oncogenes and tumour suppressors are directly regulated by Pro-directed phosphorylation and/or can trigger signalling pathways involving Pro-directed phosphorylation. PIN1 has been shown to play a critical role during oncogenesis process and it is overexpressed in the majority of cancers and acts as a modulator of several cancer-driving signalling pathways. Different groups showed that PIN1 regulates the oncogenic programme of the cells by activating more than 40 oncogenes and growth enhancers, and inactivating more or less 20 tumor suppressor and growth inhibitors (Fig. 4). PIN1 is pivotal for determining the outcome and duration of different signalling pathways by regulating numerous critical cancer-driving receptors and intracellular signalling regulators. For example, c-MYC, NOTCH1 and WNT/b-catenin interacts with Pin1 and curbs several tumour suppressors.

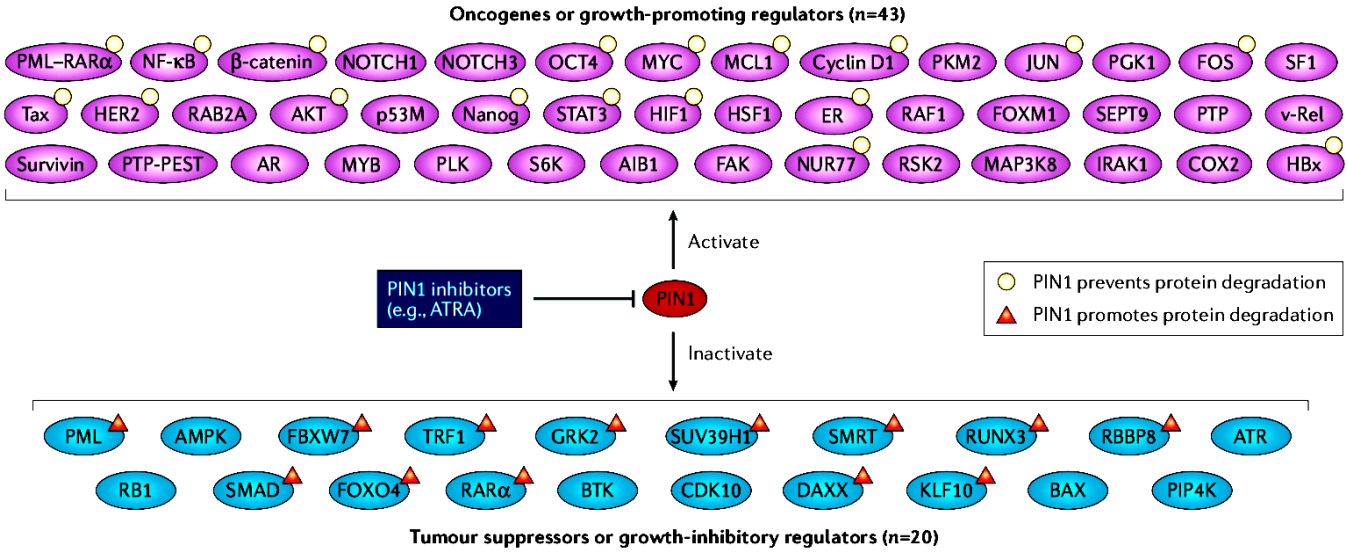

Fig.4 PIN1 promotes cancer cells by activating numerous oncogenes and growth enhancers, and inactivating numerous tumour suppressors and growth inhibitors[16].

Others example of Pin1 regulated cancer-driving receptors include HER2, NOTCH3, oestrogen receptor α (ERα) and androgen receptor (AR). Examples of PIN1-mediated intracellular signalling

regulators include RAF1, AKT, the M2 isoform of pyruvate kinase (PKM2), MYC, SMAD2 and SMAD3, signal transducer and activator of transcription 3 (STAT3), AMP-activated protein kinase (AMPK; also known as PRKAA2), the RAS family member RAB2A, focal adhesion kinase (FAK), protein tyrosine phosphatase, non-receptor type 12 (PTP-PEST; also known as PTPN12), ribosomal protein S6 kinase (S6K; also known as RPS6KB1) and serum/glucocorticoid regulated kinase 1 (SGK1). Importantly, PIN1 often acts on many signalling pathways at multiple levels to promote tumorigenesis synchronously, as demonstrated in the HER2–RAS–RAF1–MEK–ERK pathway.

Interesting the study reported by Del Sal, related to breast cancer, in which is shown the strongly interaction and cooperation between PIN1 and the mutant p53. The tumour suppressor p53 is important in the cell decision to either arrest cell cycle progression or induce apoptosis in response to a variety of stimuli. p53 post-translational modifications (phosphorylation) and association with other proteins have been implicated in the regulation of its stability and transcriptional activities [31,32]. On DNA damage, p53 interacts with PIN1 regulating the function of many proteins involved in cell cycle control and apoptosis. This interaction is strictly dependent on p53 phosphorylation (Fig 5).

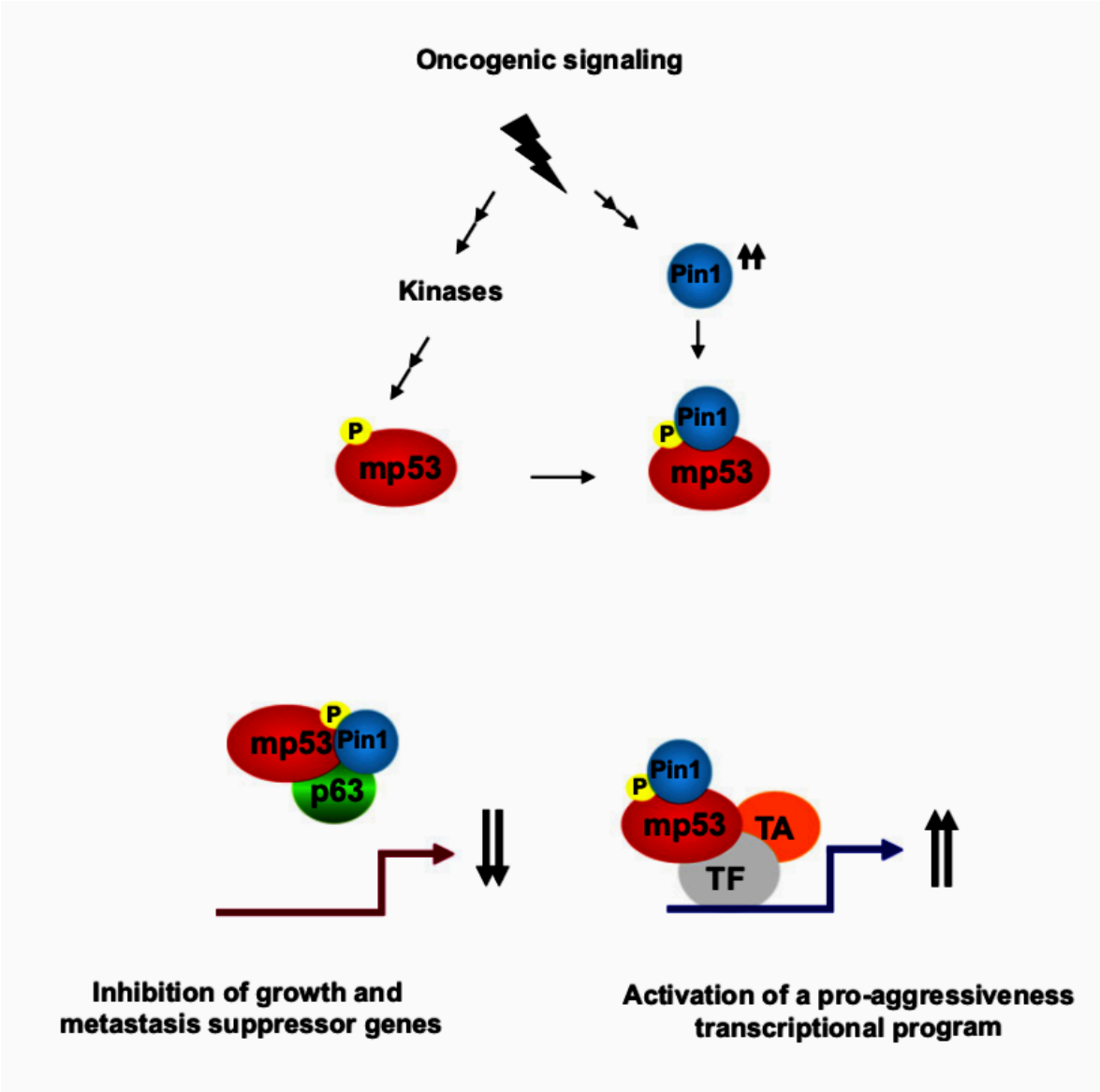

Fig.5 Pin1 amplifies mutant p53 gain of function[32].

In presence of an oncogenic signalling, the mutant p53 (mp53) is phosphorylated on specific residues: these phosphorylations are essential for the PIN1 binding. Subsequently the complex mp53-Pin1 binds and inhibits the p63 inhibiting the tumor suppressor genes and/or forming a complex with different transcriptional factors activates a pro-aggressiveness transcriptional program. [32]

With a few exceptions (such as neurons, in which PIN1 expression is induced upon neuronal differentiation), PIN1 expression is generally correlated with cell proliferative potential in normal

human tissues, but is further up-regulated in many human cancers [33,34,35]. Recent studies have demonstrated that PIN1 is prevalently overexpressed in human cancers, that PIN1 overexpression is correlated with poor clinical outcome of patients with cancer and that PIN1 has a pivotal role in multiple oncogenic signal pathways [36,37] . It has been shown that in human breast cancer cell lines and cancer tissues PIN1 is overexpressed and plays a critical role in the transformation of mammary epithelial cells by activating multiple oncogenic pathways. Furthermore, PIN1 expression is recently considered as an excellent independent prognostic marker in prostate cancer.

The PIN1 overexpression disrupts cell cycle coordination and leads to chromosome instability and tumorigenesis, promote cell proliferation and malignant cell transformation. During cell cycle progression, PIN1 is involved in the modulation of different functions of its interacting proteins through PIN1-mediated isomerization. Therefore it is normal that PIN1 expression level is crucial for the regulation of cell cycle progression. For example, several studies have demonstrated that PIN1 overexpression results in increased cell proliferation in hepatocellular carcinoma (HCC) cells [38–40]. Suizu et al. has showed that PIN1 overexpression enhances the colony formation ability in soft agar and thereby contributes to cell transformation [41]. Also, how reported in literature PIN1 depletion in HCC cells inhibited tumour growth and enhanced tumour apoptosis *in vivo* [38,40]**.** In addition, a positive association between PIN1 expression and tumour progression is further validated in various types of human cancers including brain, breast, cervical, colon, liver and prostate [25,42–44]. As a result, deregulation of PIN1 expression through different mechanisms has been studied in cancer. Numerous studies have demonstrated that depletion of PIN1 not only reduced cell proliferation, but also enhanced cellular apoptosis *in vitro* and induced tumour shrinkage in various types of cancer cells *in vivo*. Ryo *et al.* have shown that inhibition of PIN1 by overexpression of dominant-negative PIN1 mutant reduced cell proliferation and reversed transformed phenotypes on human breast epithelial cells while suppression of PIN1 expression by RNA interference reduced tumourigenicity and angiogenesis in xenograft mouse model of prostate cancer [45,46].

Consistent with a role of PIN1 in cell growth regulation, Pin1 knockout mice displayed a range of cell proliferative abnormalities, including decreased body size, testicular atrophy, retinal degeneration, and neurological abnormality. Moreover, in $Pin1^{-/-}$ adult female mice the breast epithelial compartment failed to undergo the massive proliferative changes associated with pregnancy, indicating that Pin1 is critical for cell proliferation *in vivo.*

In summary, PIN1 accelerates the conversion of cis and trans isomers: the net result on cancer cells is the activation and inactivation of more than 40 oncogenes and 20 tumor suppressor genes, respectively [16,31,47–53]. In cancer, PIN1 is overexpressed and/or over-activated, and high level of overexpression and/or over-activation correlates with poor clinical prognosis. Therefore, PIN1 inhibitors are attractive therapeutic agents for the treatment of cancers.

1.3 Pin1 inhibition

Pin1 possesses many unique features, which are attractive as therapeutic target: a) the PPIase domain has a specific, structurally-organized shaped active site that is suitable for drug development [54]; b) mice knocked down (KD) for Pin1 are viable without gross abnormalities [55] and c) genetic manipulation of Pin1 in several oncogene-induced mouse models of tumorigenesis limits tumor burden and metastatic spread [56]. Pin1 is expressed at low levels in normal tissues and specifically up-regulated in cancer cells and cancer stem cells, a subclass of neoplastic cells found in most tumors which are more resistant to multiple commonly used chemotherapeutic treatments [57]. Furthermore, inhibition of Pin1 sensitizes cancer cells to targeted- and chemo-therapies and reverse drug resistance [58,59].

In the last 10 years, different groups and companies worked in order to define Pin1 inhibitors able to block and inhibit the protein not only in vitro but also in vivo. The researchers starting their investigation looking to the inhibitors of others PPIase such as cyclosporin A, FK506 and rapamycin but it was seen that they do not inhibit PIN1.

Different classes of PIN1 inhibitors with both covalent and non-covalent binding mechanism have been developed and discovered using PPIase assays, binding assays, structural similarity or phenotypic association to PIN1 inhibition, structure-based design, substrate-mimicking design and a mechanism-based high-throughput screen.

The first identified compound that inhibits PIN1 activity is **Juglone** (Fig.6), discovered by low-throughput PPIase screens that inhibit parvulin- and Pin1-type PPIases.

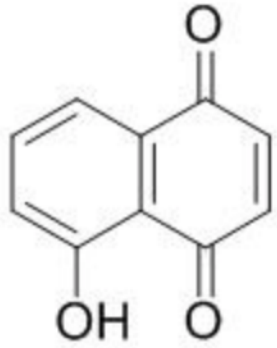

Fig.6 *Chemical structure of Juglone*

Juglone has been demonstrated to inhibit PIN1 activity and suppress cell proliferation in various types of cancers including glioblastoma, HCC, and prostate cancer [60–62]. Juglone is an irreversible Pin1 inhibitor which binds the catalytic domain PPIase and it was also demonstrated that a high concentration of Juglone (10–20 μM) reduced PIN1 protein expression [60,63]. In the mouse model study, intraperitoneal injection of Juglone inhibits tumour growth of prostate cancer [61]. Although Juglone is effective against cancer cell proliferation *in vitro* and *in vivo*, but the lack of PIN1 specificity limits its potential use in cancer treatment. In fact, Juglone also covalently modifies active site Cys in many other enzymes.

Through screening of different chemical compound libraries, several research groups also have identified specific compounds that compete for the binding to the PIN1 PPIase domain and thus inhibit PIN1 activity. Both **PiB** and dipentamethylene thiuram monosulfide (**DTM**) are found to exert anti-proliferative effect on human colon cancer cells by inhibiting PIN1 activity [64,65]. Also, through low-throughput screening for peptide that binds PIN1 has identified another PIN1 inhibitor: **pTide** that is the most active at 1nM *in vitro*, but unfortunately is inactive in cells.

The structure-based rational design, instead, led to the identification of a series of peptidomimetic inhibitors of PIN1. These inhibitors often contain a phosphate or carboxylate or a phenyl imidazole core, which are needed to target the phosphate-binding pocket of the PIN1 active site. However, although these inhibitors have low nanomolar inhibiting activity *in vitro*, but they are inactive or

poorly active in cells because the negatively charged phosphate or carboxylate renders these inhibitors cell impermeable.

Lack of cell permeability is a common problem in the pursuit of PIN1 inhibitors. In 2009, Guo and co-workers started for Pfizer a PIN1 program in order to discover new PIN1 small molecule inhibitors: the researchers, taking advantage from the similarity between the active sites of PIN1 and the peptidyl-prolyl cis-trans isomerase FKBP-12, investigated the pipecolate core that is a well-known scaffold for FKBP-12[66]. Starting from this scaffold and analyzing the PIN1 binding site, they developed different compounds, one of these with a K_i of 57 nM also providing an x-ray structure of this molecule complexed with the PIN1 enzyme [66]. Following these interesting results, the same authors tried to optimize this class of compounds in order to maintain the good enzymatic activity and to obtain activity on cell lines. Unfortunately, also these new compounds were not active in PIN1 whole cellular assays.[67,68] During the same months, Potter and co-workers from Vernalis reported similar molecules with interesting PIN1 enzymatic results [69]. Unfortunately, also these compounds were inactive in cell-based assays probably because of their low permeability.

Another newly identified PIN1 inhibitor, all-*trans* retinoic acid (**ATRA**), is an FDA approved drug used for acute promyelocytic leukemia (APL) therapy (Fig.7).

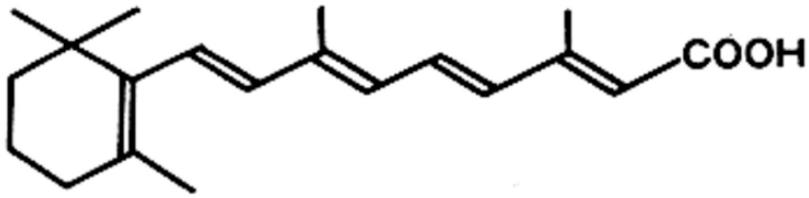

Fig.7 *Chemical structure of ATRA*

The PIN1 inhibitory activities of ATRA have been extensively studied *in-vitro* and *in-vivo* [70]. Similar to other PIN1 inhibitors, ATRA inhibits PIN1 activity by directly binding to the PIN1 catalytic PPIase domain. This binding not only induces PIN1 protein degradation, but also inhibits

the oncogenic functions of PIN1 by blocking PIN1- induced centrosome amplification and reducing cyclin D1 expression. ATRA is already approved for the treatment of acute promyelocytic leukemia (APL), which is almost caused by aberrant promyelocytic leukemia-retinoic acid receptor α (PML-RARα). In the acute myelogenous leukemia PIN1 interacts in a constitutive manner with PML-RARalpha and stabilizes it. Suppression of PIN1 by ATRA destabilizes RARalpha and PML-RARalpha, resulting in increased sensitivity to all-trans retinoic acid. The treatment of acute myelogenous leukemia cell lines with ATRA and a pharmacologic inhibitor of PIN1 causes similar effects. The slow-release formulation of ATRA that maintains ATRA plasma concentration in a steady level have been applied in *in vivo* studies as the short half-life of ATRA may reduce its anticancer efficacy against solid tumours. The slow- release formulation of ATRA has been shown to induce PIN1 degradation and reduce tumourigenicity in xenograft mouse model of breast cancer and HCC [70,71].

A more recent study by Campaner *et al.* has identified a novel PIN1 inhibitor, **KPT-6566**, with higher potency and specificity from a huge drug library of 200,000 commercial compounds [72]. KPT-6566 mediates PIN1 degradation, resulting in reduction of Rb phosphorylation and cyclin D1 expression. Unlike other PIN1 inhibitors that only exert anti-proliferative activity, KPT-6566 also possess cytotoxic effects on cancer cells through generation of reactive oxygen species. KPT-6566 induces apoptosis and inhibits cell proliferation of cancer cells including breast, prostate, lung and pancreatic cancer. KPT-6566 has also been demonstrated to exert a higher anti-proliferative effect on cancer cells than normal epithelial cells. More importantly, KPT-6566 shows growth-inhibitory effects on PIN1-expressing cells but not PIN1-silenced cells, suggesting that KPT-6566 is more specific in inhibiting PIN1 activity than the PiB that exerts growth-inhibitory effects in both PIN1-expressing and depleted cells. As for the *in vivo* study, KPT-6566 has been found to reduce the incidence of lung metastasis in mouse model of breast cancer.

In conclusion, many research groups and companies are developing PIN1 ligands; however, in spite

of highly specific molecular inhibition, they lack demonstrated effective inhibition of PIN1 and antitumor activity *in vivo*. In turn, no clinical trials have been performed due to inadequate pharmacological parameters of the developed inhibitors such as potency, solubility, and cell permeability [73].

1.4 Nanodrugs

A current approach in improving drug properties is the development of nanoparticles for drug delivery [74]. Nanodrugs retain many properties that are fundamental in cancer therapy among others:

- specific accumulation in the tumor taking advantage of enhanced permeability and retention (EPR) effect [75];
- increased therapeutic ratio (high effectiveness and low toxicity);
- improved drug solubility.

Nanoparticles have gained favour for several reasons; they offer longer systemic circulation than traditional systems and reduced clearance by the kidneys, increased drug loading capacity because of their large surface area to volume ratio, easy extravasation into tissue from leaky blood vessels (particularly in tumor vasculature), and their surfaces can be modified with various features to further enhance drug delivery[76–78]. The nanoparticle delivery efficiency can be enhanced through a number of approaches, including modifying the surface by adding targeting molecules or covalently attaching polyethylene glycol (PEG) known as PEGylation to minimize non-specific binding; changing physical characteristics such as particle size or surface charge; controlling degradation characteristics such as degradability or degradation rate and selecting materials that are sensitive to stimuli such as pH, temperature, or ionic strength.

Although thousands of nanomaterials are under investigation, liposomes, a bilayer of lipids that mimic the cell membrane are of great interest. Other than biocompatibility, these nanomaterials have already been approved by the Food and Drug Administration in the United States and the European Medicines Agency in Europe [79,80].

The liposomes have proven advantageous at solubilizing therapeutic cargos, substantially prolonging the circulation lifetimes of drugs [81]. Liposomes are small, spherical, and enclosed

compartments. If a uniform size or narrow size distribution (polydispersity < 0.2) is required, liposome size can be controlled through extrusion, through porous membranes with different dimensions, or sonication, varying the time and potency of sonication[82].

Liposomes can encapsulate different lipophilic (hydrophobic) and hydrophilic drugs: the hydrophobic drugs can be incorporated into the bilayer, while hydrophilic drugs can be contained within the inner aqueous core formed by the lipid membrane.

In general, liposomes have several attributes that make them favourable as drug carriers: they are composed by natural biodegradable lipids which are generally well-tolerated by the body, they can encapsulate a variety of drugs, and the outer surface of the liposomes can be modified to create stealth or targeted liposomes for enhanced delivery [83,84].

In clinical studies, liposomes show improved pharmacokinetics and biodistribution of therapeutic agents and thus minimize toxicity by their accumulation at the target tissue [85,86].

In 1965 Bangham discovered liposomes and in 1995 the first liposomal pharmaceutical product, Doxil®, (Ben Venue Laboratories, Inc Bedford, OH) received US Food and Drug Administration (FDA) approval (Fig.8). The liposomal formulation of Doxorubicin was utilized for the treatment of chemotherapy refractory acquired immune deficiency syndrome (AIDS)-related Kaposi's sarcoma [85–87].

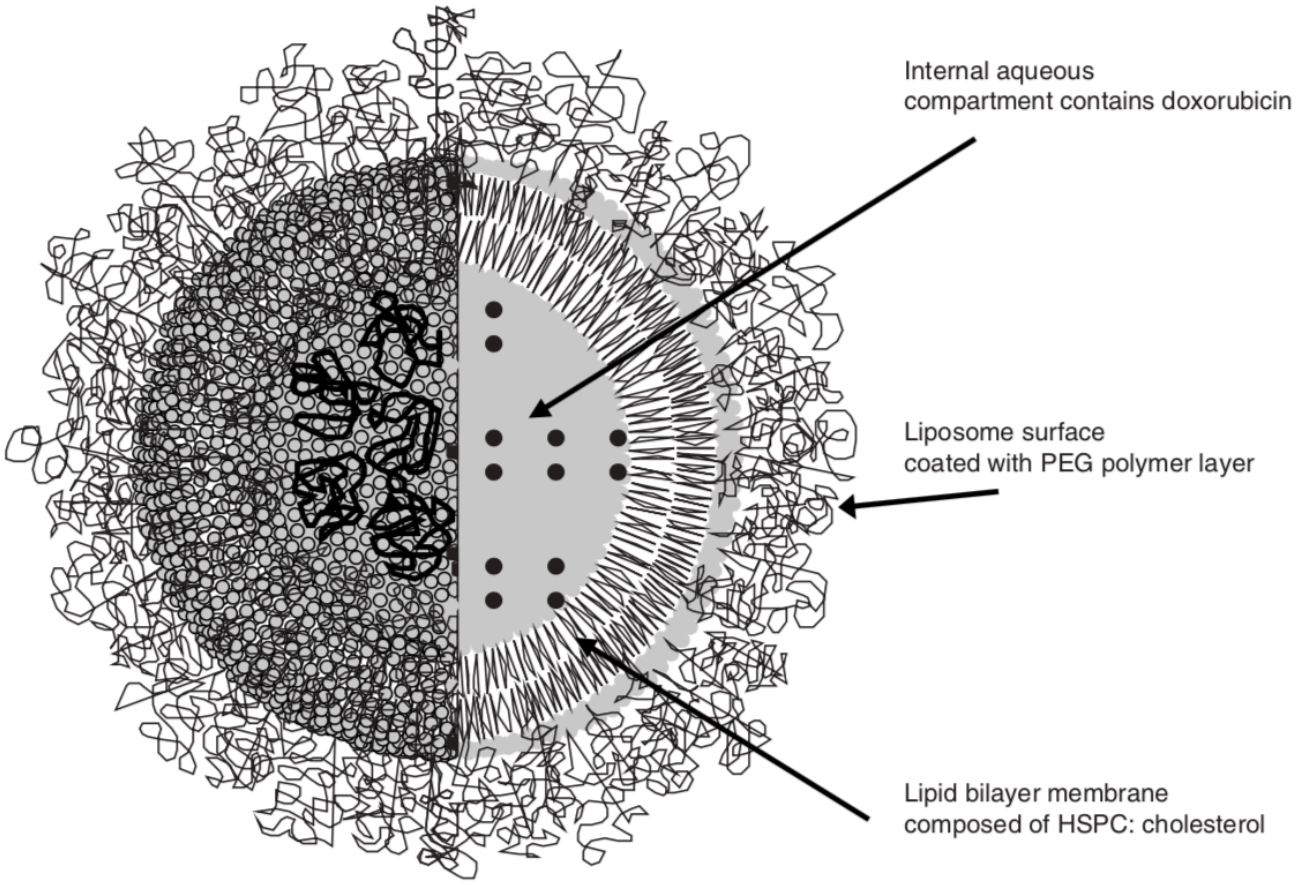

Fig.8 Liposomal formulation of Doxorubicin: Doxil [79]

Currently, there are about twelve liposome-based drugs approved for clinical use and more are in various stages of clinical trials. Most liposomal drug formulations, such as Doxil and Myocet™ (GP- Pharm, Barcelona, Spain), are approved for intravenous application [88]. Other administration routes such as intramuscular delivery have been approved for delivery of surface antigens derived from the hepatitis A or influenza virus (Epaxal® [Berna Biotech Ltd, Berne Switzerland] and Inflexal® V [Berna Biotech España SA, Madrid, Spain]). The particle size of Myocet is about 190 nm and Doxil is about 100 nm. Both liposomal products have longer circulating half-life in blood as compared with the free drug, but Doxil has a much longer circulation time in blood than Myocet. Generally, the blood circulation time of liposomes ($T_{1/2}$) increases with decreasing size, negative charge density, and fluidity in the bilayer or PEG surface coating.

The project

Departing from this state of art, I focused my attention on Pin1 expression and chemical inhibition in HGS-EOC models.

First, I confirmed that Pin1 is effectively involved in tumor progression utilizing mouse ovarian surface epithelial cancer cell line (STOSE), which closely recapitulates the characteristics of human HGS-EOC. So, I showed that comparing normal and knock down cells there is a tumor formation only in mice with Pin1 expression and activity.

Then I focused my attention in order to develop an efficient Pin1 inhibitor, able to down regulate Pin1 expression *in vitro* but also *in vivo*. Starting from the inhibitor developed by Pfizer (Fig.9), which showed a good enzymatic activity *in vitro* [89], and it's very specific for the catalytic site of the enzyme, in the last 3 years I worked in order to increase the permeability of this compound.

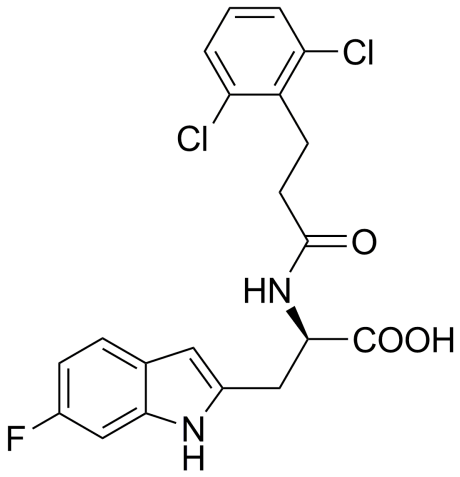

Fig.9 Pin1 inhibitor developed by Pfizer and encapsulated inside liposome by remote loading

The presence of carboxylate group permits the formation of different H-bond interactions in the proline binding site, interactions necessary for Pin1 catalytic function. Also the benzyl-imidaziole is a donator of hydrogen bonds that stabilize the interaction with Pin1. Despite significant improvements in Pin1 inhibitor affinity, these benzimidazole-based inhibitors failed to show

cellular effects (up to 100 μM) on cancer cells. The authors hypothesized that this was due to poor cell permeability caused by high polarity on the benzimidazole series.

The hydrophobic and nonionizable drugs cannot be loaded into liposomes through conventional means. In fact, ionisable hydrophilic drug can be remote loaded inside the liposomes using a transmembrane pH with efficient incorporation (Fig. 10A). The most important example is the Doxil. But a poorly soluble hydrophobic drug is not encorporated into liposomes with the same high efficacy (Fig. 10B). For this reasons, how reported from Volgestein group, the hydrophobic compound can be actively loaded into liposomes by encapsulating them into modified cyclodextrins (Fig. 10C). [90]

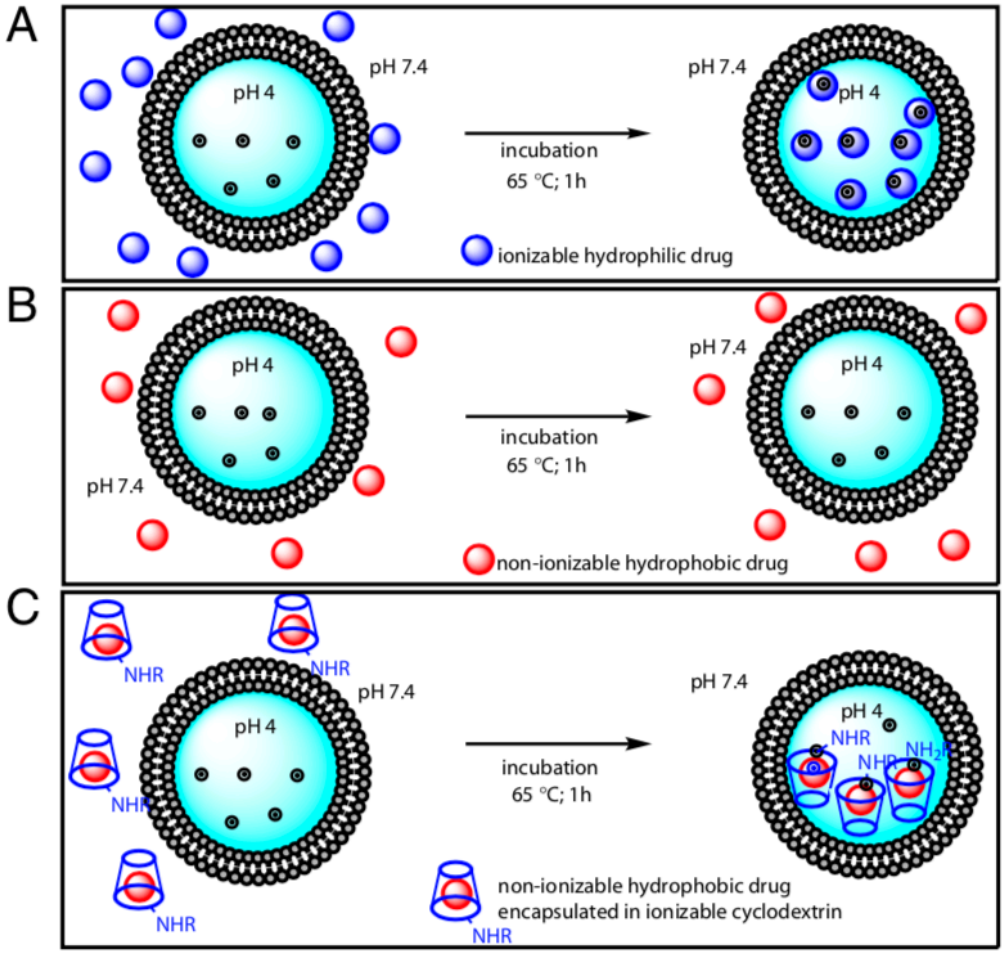

Fig.10 Schematic representations of active loading of a liposome [90]

The encapsulation of a poorly soluble drug into an ionizable cyclodextrin (preloading) enhances its water solubility and permits efficient liposomal loading via a pH gradient.

In our protocol the Pin1 inhibitor, called compound 8, is preloaded inside modified cyclodextrins, Heptakis 6ammino6deoxy cyclodextrins, and then the complex cyclodextrin-compound 8 (C8) is loaded inside the liposomes via a pH gradient. How reported in the published article, the complex liposomes-cyclodextrin-compound 8 (LC8) is able to down regulate the Pin1 level *in vitro*, reducing the vitality of cancer cells, and also had activity *in vivo*, reducing the tumor volume and the Pin1 expression [91].

2. Materials and methods

2.1 Synthesis of compound 8

A representative Pin1 inhibitor (compound **8**, Scheme S1; compound 17 in Guo *et al*., [68]), belonging to the alkyl amide indole-based library of compounds developed by Pfizer was synthesized in the laboratory of Prof.. Tiziano Tuccinardi (University of Pisa) following the reported procedure [68] .

(R)-1-Ethoxy-1-oxopent-4-yn-2-aminium chloride (**2**). Acetyl chloride (1.95 mL) was carefully added in a dropwise fashion to a flask of stirring ethanol (39 mL) at 0 °C and stirred for 30 min at room temperature. Commercially available D-propargylglycine **1** (1.00 g, 8.84 mmol) was added and the reaction was refluxed for 3h. The solvent was then removed under reduced pressure and the residue was triturated with diethyl ether to give the pure ester hydrochloride salt **2** as an off-white solid (1.52 g, 97% yield). ^{1}H NMR ($CDCl_3$): 1.32 (t, 3H, J = 7.1 Hz), 2.27 (s, 1H), 3.11 (ABq, 2H, $\delta\delta_{AB}$ = 0.15, J_{AB} = 17.4 Hz), 4.25-4.40 (m, 3H), 8.70-8.90 (m, 3H).

(R)-Ethyl 2-((tert-butoxycarbonyl)amino)pent-4-ynoate (**3**). To a cooled dichloromethane solution of **2** (12.6 mmol in 32.1 mL) triethylamine (5.3 ml) and $(Boc)_2O$ (19.0 mmol) were added and the mixture was stirred at room temperature ON. The residue was dissolved in CH_2Cl_2 and washed with 1M sodium bicarbonate, water, and brine, dried over Na_2SO_4, and concentrated. The crude product (3.66 g) was submitted to the next step without further purification. ^{1}H NMR ($CDCl_3$): 1.29 (t, 3H, J = 7.1 Hz), 1.45 (s, 9H), 2.03 (t, 1H, J = 2.6 Hz), 2.67-2.80 (m, 2H), 4.16-4.30 (m, 2H), 4.41-4.48 (m, 1H), 5.35 (br d, 1H, J = 7.7 Hz).

(R)-Ethyl 5-(2-amino-4-fluorophenyl)-2-((tert-butoxycarbonyl)amino)pent-4-ynoate (**4**). To a solution of **3** (3.47 mmol) in DMF (9.7 mL), commercially available 5-fluoro-2-iodoaniline (3.47 mmol), iPr$_2$NH (3.2 mL), $Pd(PPh_3)_2Cl_2$ (0.139 mmol) and CuI (0.278 mmol) were added and the resulting mixture was heated at 90 °C for 20 min under argon atmosphere. The mixture was cooled to RT, diluted with CH_2Cl_2, washed with water and brine and the organic phase was dried over

anhydrous sodium sulphate. Evaporation of the organic solvent under vacuum afforded a crude product, which was purified by column chromatography over silica gel (*n*-hexane/ethyl acetate 85:15), to yield pure **4** (788.6 mg, 65% yield) as a yellow oil. ^{1}H NMR ($CDCl_3$): 1.30 (t, 3H, *J* = 7.1 Hz), 1.45 (s, 9H), 2.97 (d, 2H, *J* = 4.8 Hz), 4.20-4.30 (m, 2H), 4.52-4.60 (m, 1H), 5.42 (br d, 1H, *J* = 7.1 Hz), 6.32-6.43 (m, 2H), 7.16 (t, 1H, *J* = 7.4 Hz).

(R)-Ethyl 2-((tert-butoxycarbonyl)amino)-3-(6-fluoro-1H-indol-2-yl)propanoate (**5**). CuI (2.85 mmol) was added to a DMF solution of **4** (2.85 mmol in 9.9 mL), and the mixture was stirred at 150 °C for 4 h under argon. After being cooled to RT, the mixture was filtered through a pad of celite and the filtrate was diluted with CH_2Cl_2 and washed with water and brine. The organic phase was dried and concentrated. The crude product was purified by flash chromatography over silica gel and elution with *n*-hexane/EtOAc (8:2) afforded the desired compound **5,** (739.5 mg, 74% yield) a brown solid. ^{1}H NMR ($CDCl_3$): 1.24 (t, 3H, *J* = 7.1 Hz), 1.43 (s, 9 H), 3.25 (d, 2H, *J* = 5.0 Hz), 4.21 (qd, 2H, *J* = 7.1, 2.6 Hz), 4.55-4.64 (br m, 1H), 5.13-5.21 (br m, 1H), 6.24 (s, 1H), 6.84 (ddd, 1H, *J* = 9.7, 8.6, 2.3 Hz), 7.00 (dd, 1H, *J* = 9.6, 2.3 Hz), 7.42 (dd, 1H, *J* = 8.6, 5.4 Hz), 8.44 (br s, 1 H).

(R)-Ethyl 2-amino-3-(6-fluoro-1H-indol-2-yl)propanoate (**6**). Compound **5** (2.54 mmol) was dissolved in CH_2Cl_2 (11.4 mL), cooled to 0 °C, treated with trifluoroacetic acid (3.43 mL), and stirred at RT for 2 h. The mixture was concentrated to dryness under reduced pressure, diluted with EtOAc, and washed with 1 M solution $NaHCO_3$ and brine, and then the organic layer was dried over Na_2SO_4 and concentrated. The crude product was purified by flash chromatography over silica gel. Elution with $CHCl_3$/MeOH (98:2) gave the pure compound (530 mg, 83% yield) as a light yellow solid. ^{1}H NMR (CD_3OD): 1.17 (t, 3H, *J* = 7.1 Hz), 3.03 (dd, 1H, J = 14.5, 7.2 Hz), 3.15 (dd, 1H, *J* = 14.5, 5.9 Hz), 3.79 (dd, 1H, *J* = 7.3, 6.1 Hz), 4.14 (q, 2H, *J* = 7.1 Hz), 6.21 (d, 1H, *J* = 0.8 Hz), 6.73 (ddd, 1H, *J* = 9.9, 8.6, 2.4 Hz), 6.98 (dd, 1H, *J* = 9.9, 2.4 Hz), 7.37 (dd, 1H, *J* = 8.6, 5.1 Hz).

(R)-Ethyl 2-(3-(2,6-dichlorophenyl)propanamido)-3-(6-fluoro-1H-indol-2-yl)propanoate (**7**). HATU (1.05 mmol) was added to a solution of commercially available 3-(2,6-

dichlorophenyl)propionic acid (0.999 mmol) in dry DMF (4.6 mL), then DIPEA (0.70 mL) was added in a dropwise fashion. The resulting mixture was stirred at room temperature for 30 min, and then compound **6** (0.999 mmol) was added and left under stirring at room temperature for 6h. After this time, the residue was diluted with water and extracted with EtOAc. The organic layer was washed sequentially with water and brine and dried over Na_2SO_4 and the solvent was removed under reduced pressure. The residue was purified with flash column chromatography (*n*-hexane/ethyl acetate 7:3), and pure fractions containing the desired compound were evaporated to dryness. Compound **7** was obtained as a light yellow solid (406.2 mg, 90% yield). ^{1}H NMR (DMSO-d_6): 1.09 (t, 3H, J = 7.1 Hz), 2.29-2.35 (m, 2H), 2.98-3.19 (m, 4H), 4.06 (qd, 2H, J = 7.1, 1.3 Hz), 4.58-4.66 (m, 1H), 6.19 (d, 1H, J = 1.2 Hz), 6.78 (ddd, 1H, J = 10.0, 8.6, 2.4 Hz), 7.06 (dd, 1H, J = 10.0, 2.5 Hz), 7.26 (dd, 1H, J = 8.5, 7.6 Hz), 7.39 (dd, 1H, J = 8.7, 5.5 Hz), 7.43 (d, 2H, J = 8.2 Hz), 8.42 (d, 1H, J = 7.6 Hz), 11.07 (s, 1H).

(R)-2-(3-(2,6-Dichlorophenyl)propanamido)-3-(6-fluoro-1H-indol-2-yl)propanoic acid (**8**). Ethyl ester **7** (0.526 mmol) was dissolved in MeOH (6.0 mL), cooled to 0 °C, and treated with 3.0 mL of aqueous NaOH 5% w/v. The reaction was stirred at RT for 1.5 h then the solvents were evaporated and the residue was diluted with water and washed with Et_2O. The aqueous phase was acidified with 1 N aqueous HCl and the extracted with EtOAc. The organic phase was dried and evaporated to yield the pure desired carboxylic acid derivative **8** as an off-white solid (370 mg, 99% yield). ^{1}H NMR (DMSO-d_6): 2.27-2.36 (m, 2H), 2.98-3.08 (m, 3H), 3.18 (dd, 1H, J = 14.7, 5.8 Hz), 4.32 (q, 1H, J = 6.4 Hz), 6.15 (s, 1H), 6.74 (ddd, 1H, J = 10.0, 8.6, 2.0 Hz), 7.05 (dd, 1H, J = 10.4, 2.3 Hz), 7.25 (dd, 1H, J = 8.5, 7.6 Hz), 7.34 (dd, 1H, J = 8.5, 5.5 Hz), 7.42 (d, 2H, J = 8.1 Hz), 7.77 (br d, 1H, J = 7.4 Hz), 11.19 (s, 1H). ^{13}C NMR (DMSO-d_6): 26.99, 30.76, 33,34, 53.58, 96.82 (d, J = 26.2 Hz), 99.49, 106.49 (d, J = 24.1 Hz), 119.64 (d, J = 10.1 Hz), 125.04, 128.42 (2C), 128.75, 134.38 (2C), 135.66 (d, J = 12.1 Hz), 136.59, 137.92, 158.10 (d, J = 232.4 Hz), 169.82, 170.45.

2.2 Liposomal formulation

Pegylated liposomes: 1,2-distearoyl-*sn*-glycero-3-phosphocholine **(**DSPC), cholesterol, and 1,2-dipalmitoyl-*sn*-glycero-3-phosphoethanolamine-N-[methoxy(polyethylene glycol)-2000 **(**DPPE-PEG) from Avanti Polar Lipids (50:45:5, molar ratio) were dissolved in chloroform (20 mL). The solvent was removed by vacuum to form a thin lipid film, which was hydrated by shaking in the appropriate buffer (80 mM Arg·Hepes, pH 9.0) at 65 °C for 2 h. The vesicle suspension was serially extruded through 0.4-, 0.2- and 0.1- μm polycarbonate membranes (Whatman; Nuclepore Track-Etched Membrane) at 65°C to obtain mono-dispersed liposomes. A transmembrane gradient was created by an ON dialysis in PBS. The average size and polydispersity index were measured by dynamic light scattering experiments on a Zetasizer Nano ZSP (ZEN 5600-Malvern Instruments, Malvern, UK).

Cyclodextrin-Inhibitor (CI) complex: compound **8** was dissolved in methanol and mixed with equimolar quantity of Heptakis-(6-amino-6-deoxy)-β-Cyclodextrin 7xHCl (CDexB-013; Arachem, Netherlands) in deionized water. In detail, the methanolic solution of the drug was added in a dropwise fashion to the cyclodextrin solution in agitation (final concentration of methanol was 10%). This suspension was shaken at 55 °C for 48h. The solution was flash-frozen in a dry ice/acetone bath followed by lyophilization and then stored at −20 °C until further use.

Liposomes/cyclodextrin/compound **8** complex: After lyophilization, CI was incubated with 20mg/mL of liposomal solutions for 1h at 65 °C. The sample was spun at maximum speed in order to remove the particulate matter. The amount of inhibitor loaded within the liposomes was determined by UV-Visible method utilizing a calibration curve (NanoDrop 2000c; Thermo Fisher Scientific, Waltham, MA, US). The inhibitor and LC8 were dissolved in methanol and analyzed at 270 nm.

2.3 Loading and release

The loading of inhibitor was evaluated with the UV-VIS method using the NanoDrop 2000c instrument after disruption of the liposomal solution with methanol: 5µl of LC8 was dissolved in 600µl of methanol. The inhibitor presents a characteristic peak at 270 and 290 nm. The release of inhibitor (1 mg/ml) was evaluated from dialysis membrane (Slide-A-Lyzer® MINI Dialysis Devices, 20K MWCO), at 37 °C, in PBS 1X.

2.4 Half maximal inhibitory concentration (IC_{50})

In order to evaluate the IC_{50} of inhibitor and inhibitor loaded inside the liposomes (LC8), cells were plated in a 96-well plate one day before treatment (OVCAR3: 10^3 cells/well; MRC-5 10^4 cells/well). Then the cells were treated with inhibitor, LC8, and empty liposomes starting with a concentration of 100µM followed by five 1:2 serial dilutions. After 96h, the cell viability was evaluated by CellTiter-Glo® Luminescence assay (Promega, Madison, Wisconsin, US) with the Infinite 200 PRO instrument (Tecan) and IC_{50} was calculated using the GraphPad program (Prism, CA, US).

2.5 Pin1 targets and western blot analysis

T47D, PLC/PRF/5 and OVCAR3 cells were seeded with a density of $5X10^5$ in 100 X 20 mm tissue culture dish (Falcon® Corning Brand) one day before treatment. The cells were treated with liposomal/cyclodextrin/compound **8** (LC8) 100 µM and with ATRA 10 µM for 24h then the cells were collected for western blot analysis. $3x10^5$ NIH3T3 cells were plated one day before treatment. Cells were treated with 0, 50 and 100 µM of LC8, collected after 48h and analyzed by RT-PCR or

cells were treated with 100 μM of LC8 and DMSO as control for 24h followed by 10μg/mL of CHX. Cells were collected after 0, 3, 6, 12 and 24h for western blot analysis. Cells were also treated with 0, 50 and 100 μM of LC8 for 48h and then treated with MG132 10 μM and after 6h collected for western blot analysis. Quantification analysis was done with Image J software.

2.6 Animal studies

Animal studies were done in accordance to the Italian Governing Law (D.lgs 26/2014) under the authorization of Ministry of Health n° 788/2015-PR and performed in accordance with the institutional guidelines. Data are reported as the mean and standard error.
Immunocompetent tumor model: 10^7 STOSE cells were injected i.p. into 8-week-old female FVB/N mice (Envigo, UK).

Immunodeficient tumor model: $5x10^6$ OVCAR3 cell line were mixed with DMEM w/o phenol red/50% of Cultrex® Basement Membrane Matriz, Type 3 (Trevigen) and implanted subcutaneously into the flank of 6-week-old female nude mice (Envigo, UK). When tumors reached a measurable size, mice were treated i.p. with LC8 one time per week for three treatments. Tumor volumes were measured with a caliper and calculated using the formula: $(length \times width^2)/2$. PK: the experiment was performed in 8 weeks old FVB/N mice (Envigo, UK) treated with 20mg/kg (i.p.) of the drug diluted in PBS 1X. A hundred μl of blood was collected after 0.16, 3, 6, 12 and 24h and analyzed by liquid chromatography tandem mass spectrometry (LC-MS/MS). A total of 200 μl were drawn from each mouse.

Biodistribution: female nude mice (Envigo, UK) were treated at a dose of 20mg/kg and sacrificed after 72h. The organs were washed with 10ml of cold PBS/heparin before collection, diluted in 500

µl of PBS/BSA 4%, and homogenized with Qiagen Tissue Ruptor for 20 s at power 4 in ice. Samples were stored at -80 °C. The concentrations of inhibitor were measured by LC-MS/MS.

2.7 LC-MS/MS

Before extraction, a known amount of internal standard (IS) solution (Guo *et al*., [68], compound 16) was added to PK and biodistribution samples. Then, acetonitrile/0.1 % formic acid was added (final volume ratio, 1:2); samples were vortexed and placed into a sonicator bath for 5 min at 4° C. This procedure was performed twice and after centrifugation (14000 rpm, 20 min, 4° C), supernatants were collected together and dried under vacuum (Univapo 150 H). Calculated extraction recoveries are reported in Table S1. Five-point calibration curves within the analyte concentration ranges 0.6–2857.1 ng/ml and 0.2–95 ng/ml were prepared in blank serum and tissue samples, obtained from untreated mice.

LC-MS/MS analysis was performed with an UltiMate 3000 system (ThermoFisher Scientific, CA, USA) coupled to an API 4000 triple quadrupole mass spectrometer (AB SCIEX, Massachusetts, USA) working in multiple reaction monitoring (MRM) modality. Selected transitions for Compound **8** and IS were as follows: m/z 423.1 > 206.1 and m/z 423.1 > 218.1 for Compound **8**; m/z 391.1 > 206.2 and m/z 391.1 > 188.1 for IS. The optimized ESI (+) source parameters are reported in Table S1. Chromatographic separation was performed on a Hypersil GOLD C8 column (2.1 × 100 mm, 3 µm, ThermoFisher Scientific). Elution was achieved by a linear gradient (mobile phase A: 0.1 % formic acid, mobile phase B: acetonitrile/0.1 % formic acid) from 30 % to 95 % B over 4 min. Injection volume was 10µl and flow rate was 300µl/min.

2.8 Statistical analysis

The statistical significance was determined using the two-tails paired t-test, unless specified. A p-value less than 0.05 were considered significant for all comparisons done.

3. Results

3.1 Pin1 knock-down reduces tumor cell growth

To understand if Pin1 is a valid therapeutic target in HGSOC, we knocked down its expression in a spontaneously transformed mouse ovarian surface epithelial cancer cell line (STOSE), which closely recapitulates the characteristics of human HGSOC [92].

Firstly Pin1 activity was evaluated and Fig.11 shows the western blot analysis. Mouse shRNAs efficiently down-regulate (kd) and up-regulate (HaPin1) Pin1 protein in STOSE cells.

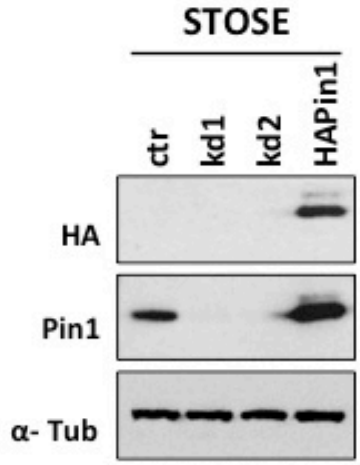

Fig.11 Pin1 knock-down in vivo in a syngeneic model of HGSOC.

Since STOSE cell lines derived from FVB/N mice (syngeneic), normal and knock down cells were injected intraperitoneally (i.p.). Fig. 12 demonstrates that Pin1 KD abolishes tumor formation after 3 months.

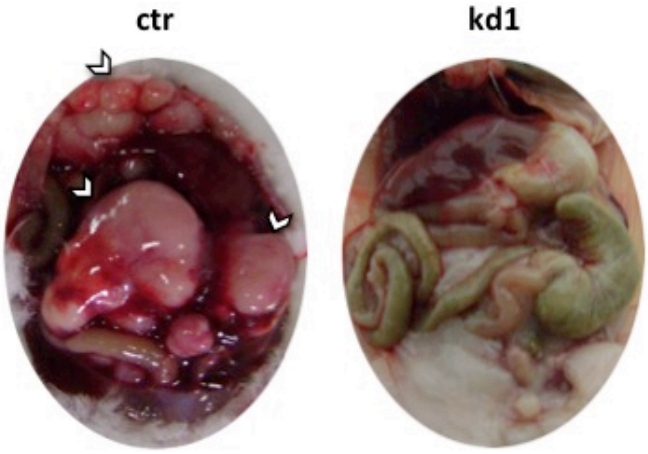

Fig.12 FVB/N mice injected with STOSE cells wild type or kd for Pin1 (n=3)

The mice injected with wild type cells (ctr) present tumor formation in the peritoneal cavity compared to the knock down (kd1). These results are in accordance with the evidences reported in literature: the high-grade serous ovarian cancer, in fact, is characterized by spreading of cancer cells in the peritoneal cavity where the cells are able to invade the organs within the peritoneal cavity.

The STOSE cells in which Pin1 expression is down regulate loss the capability to form tumors and invade the peritoneal cavity.

3.2 Liposomal/cyclodextrin/compound8 (LC8) has desired pharmacological properties

Liposomal nanoparticles have been successful utilized as treatments for different diseases [93]. The major advantages are biocompatibility and an improved therapeutic window [94]. Unfortunately, only weakly acidic or basic drugs could be stably incorporated inside the cores of liposomes [95]. Recently, the Vogelstein group demonstrated that a hydrophobic drug could be solubilized in physiologic buffers and remote loaded into liposomes by modified cyclodextrins that have the properties of weak bases or acids [90].

A representative Pin1 inhibitor (compound **8**, Fig.13), belonging to the alkyl amide indole-based library of compounds developed by Pfizer, was synthesized in our laboratory, since it was among the most potent inhibitors of the isolated enzyme, showing a *Ki* value of 75 nM. This compound could be easily synthesized but it has a low solubility profile in water and is ineffective on cancer cells [66,68,89].

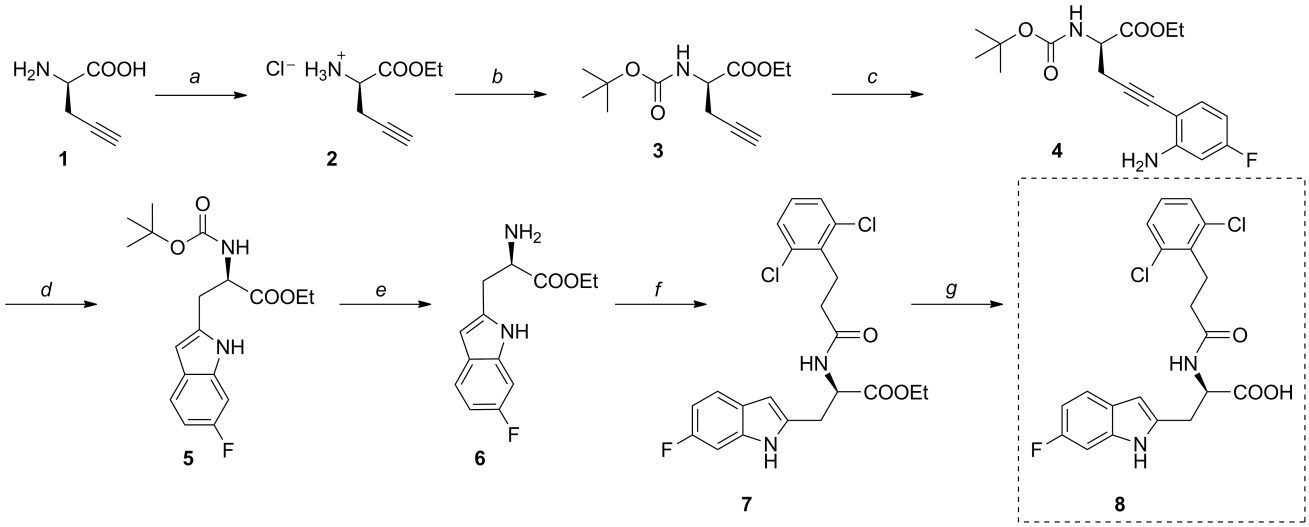

Fig. 13 Synthesis of compound 8: reagents and conditions. (A) EtOH, AcCl, reflux; (B) $(Boc)_2O$, Et_3N, DCM RT; (C) CuI, $Pd(PPh_3)_2Cl_2$, iPr_2NH, DMF, 90 °C; (D) CuI, DMF, 150 °C; (E) TFA,

DCM, RT; (F) 3-(2,6-dichlorophenyl)propionic acid, HATU, DIPEA, DMF, RT; (G) NaOH 5% w/v, MeOH, RT.

Compound **8** was solubilized in Heptakis (6-ammino-6-deoxy)-β-cyclodextrins and loaded into pegylated-liposomes (Fig. 14A: schematic representation of the active loading). Compound **8** has a solubility of 0.30± 0.05 mg/ml in PBS. When formulated as a liposomal/cyclodextrin complex (Fig. 14B), the solubility of the Pin1 inhibitor increased by about 6 times (1.82±0.10 mg/ml) (Fig. 14B). The presence of cyclodextrins permits the solubilisation of the compound **8** and the encapsulation in an ionisable vehicle. The presence of amino groups on the surface of the cyclodextrins permits subsequently the encapsulation inside the liposomes via a pH gradient.

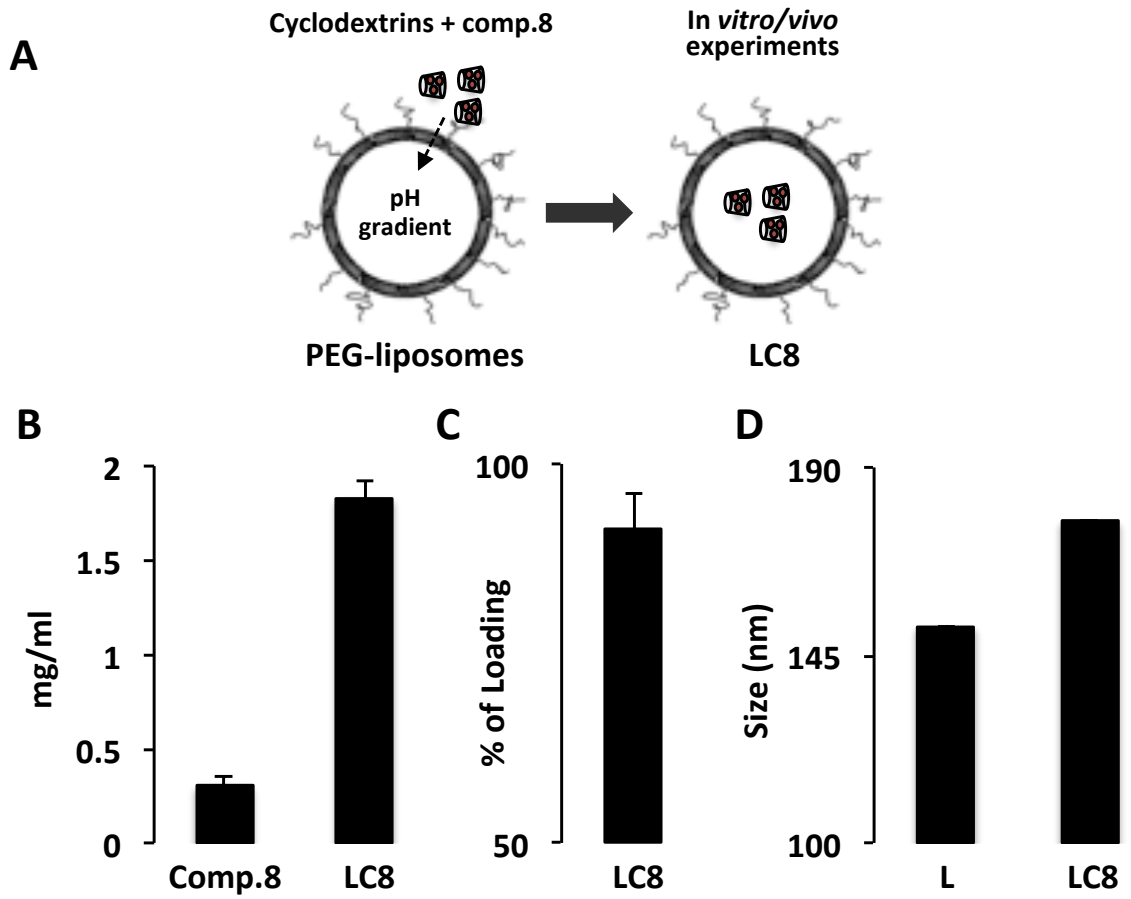

Fig. 14 Liposomal/cyclodextrin/compund8 (LC8): chemical-physical properties and in vitro activity. (A) Schematic representation of the active loading of compound 8 (Comp.8) into pegylated

liposomes. (B) LC8 increases the solubility of comp. 8 in PBS solution by about 6 times. (C) The loading efficiency of comp. 8 into pegylated liposomes is more than 90%. (D) DLS analysis of liposomes before (L) and after loading of LC8.

The loading efficiency of LC8 was evaluated by UV absorbance: the inhibitor present two characteristic peaks of absorbance, in this investigation I considered the peak at 270nm. The loading efficacy was of 91.2±5.0 percent, and was calculated considering the ratio between the quantity of drug loaded / total drug (Fig. 14C). Analysing the measures of liposomes pre and post loading, the data showed a low polydispersity index with the size of liposomes that increase from 151.8±0.10 nm (pre) to 177±0.11 nm (post) (Fig. 14D). This data confirmed an effective loading of the complex cyclodextrin/compound **8** inside the liposomes.

The hydrodynamic size of liposomes was also evaluated under different temperatures using the DLS. The size increased from 25 to 37 °C and remained stable up to 65 °C (Fig. 15).

z-average	PdI	Temperature (°C)
129.1	0.048	25
144.3	0.079	37
142.9	0.032	45
146	0.055	60
143.1	0.055	65

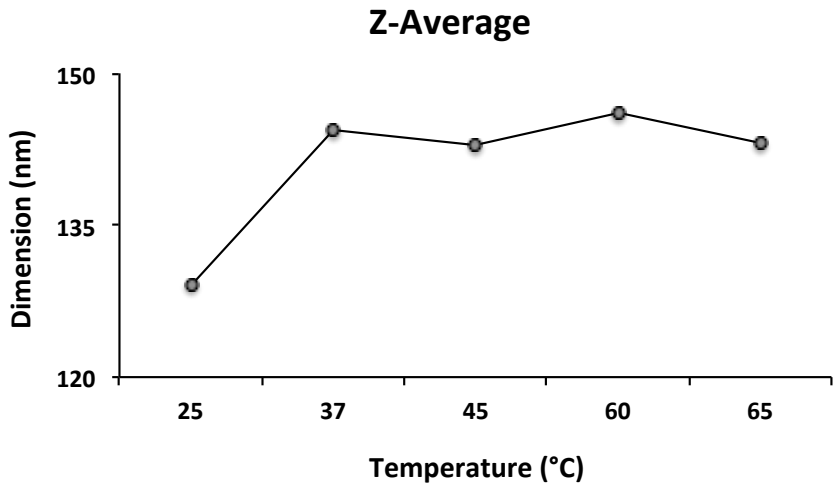

Fig. 15 DLS analysis of hydrodynamic size of liposomes at different temperatures.

The ability of LC8 to retain compound **8** was then tested with a release assay. Fig. 16 demonstrates that the release from a semipermeable membrane of LC8 was slower than inhibitor alone (Comp.**8**). The liposomal formulation permits the effectively accumulation and retaining of compound **8** into the liposomes thanks to the presence of cyclodextrins.

The slow release rate may contribute to the change the *in vivo* pharmacological properties.

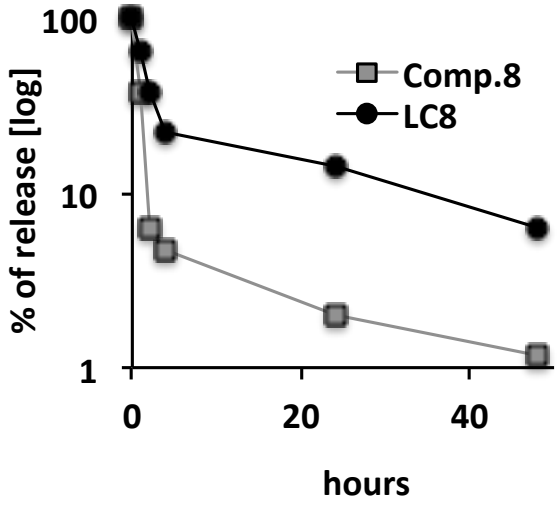

Fig. 16 Release of comp. 8 or LC8 through a semipermeable membrane. Representative result.

As proof of concept, LC8 was tested on OVCAR3 cells. Although compound **8** has no activity, how reported from Pfizer, LC8 has an IC_{50} value in the low micromolar range (Fig. 17).

OVCAR3	IC50 (µM)	sDev
LC8	21.3	5.9
Cyclodex+ Comp. 8	NA	
Lcomp. 8	NA	
Comp. 8	NA	
L	NA	

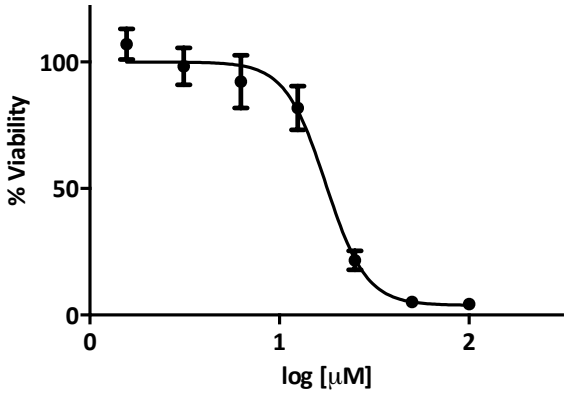

Fig. 17 OVCAR3 cell line was treated with LC8, cyclodextrin/comp. 8, liposome/compound 8, comp. 8, or empty liposomes (L) and the IC50 was determined after 96 hours (NA: Not applicable). Representative IC50 dose-response curve of OVCAR3 cells treated with LC8.

LC8 has no activity on MRC-5 normal fibroblasts (data not shown) demonstrating no toxic effects on normal cells. These results allowed us to test LC8 in an *in vivo* mouse model.

3.3 LC8 promotes Pin1 protein degradation

High affinity or covalent inhibitors promote degradation of Pin1 [71] [72]. To assess the effect of LC8, fibroblast cells (NIH 3T3) were treated with 100 μM of LC8. At the mRNA level, the LC8 treatment did not substantially alter Pin1 (Fig. 18B) and the LC8 had no obvious effects on Pin1 mRNA levels.

But, we observed that LC8 caused a decrease in the level of the Pin1 protein (Fig. 18A) after 48 hours of treatment. To discriminate between protein degradation and decreased stability, cells were also treated with MG132 (proteasome inhibitor) for 6 hours (Fig. 18A) or CHX (protein synthesis inhibitor) for indicated time points (Fig. 18C).

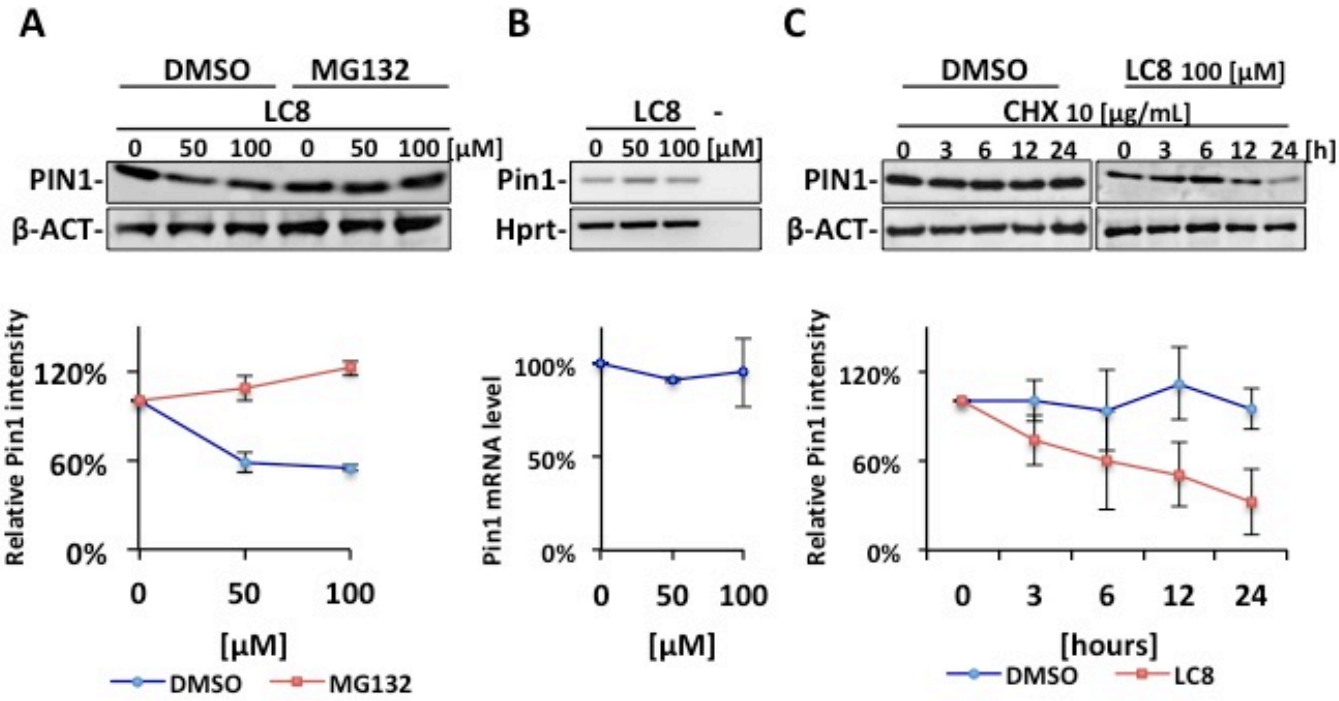

Fig. 18 LC8 induces Pin1 degradation through the proteasome. (A) Fibroblasts were treated with 100 μM of LC8 for 48 hours followed by 10 μM of proteasomal inhibitor MG132 for 6 hours. MG132 was abled to rescue the expression of Pin1 protein. (B) Fibroblasts were treated as in (A).

Pin1 RNA levels was unaffected. (C) Fibroblasts were treated with 100 μM of LC8 for 24 hours followed by 10 μg/ml of CHX for the indicated time. LC8 induces protein degradation through the proteasome. Bottom panel: semi-quantitative analysis was reported (three independent experiments).

Only MG132 rescued the expression of Pin1 confirming a specific mechanism of protein degradation mediated by the proteasome. In fact the treatment with LC8 plus CHX (Fig. 18C) only reduce the half-life of Pin1 protein, confirming as showed for ATRA by others researchers, Pin1 degradation mediated by proteasome.

In bottom panel is reported a semi-quantitative analysis of three independent experiments. The treatment with the LC8 plus DMSO for 48 hours reduce around 40% the Pin1 protein, and only the presence of MG132 is able to restore the Pin1 level. Also when the cells where treated with LC8 for 24 hours plus CHX for indicated time point, the level of Pin1 protein decrease dramatically because the LC8 inhibit the protein and the CHX block the protein synthesis. The Pin1 mRNA level was not affected by the presence of LC8, the inhibitor binds only the protein and no its RNA.

3.4 LC8 alters the levels and function of PIN1 substrates

Since Pin1 might regulate different cancer substrates in different cancer types, and also controls multiple cancer drive-pathways through regulation of many oncogenes and tumor suppressor genes at various levels [16], the inhibition of Pin1 by chemical ablation would affect protein levels of a selected set of Pin1 substrates or downstream factors

We utilized T47D (breast) and PLC/PRF/5 (liver) cancer cell lines as published models and OVCAR3 cell line to study LC8's effect [96,97].

The three different cell lines were treated for 24 hours with 100 μM of LC8 and as a positive control we utilized ATRA, a recently published inhibitor of Pin1[63]. The protein stability and abundance of Pin1 target proteins results altered after chemical inhibition of Pin1. Compared to untreated cells, LC8 down-regulated the expression of β-catenin, LC3B (autophagy), and cyclin D1 (cell cycle; only in T47D cells) (Fig. 19).

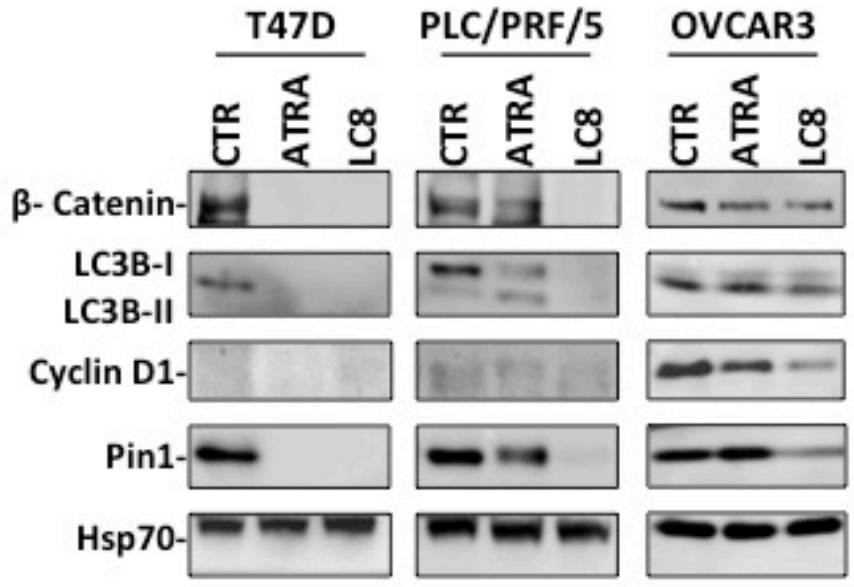

Fig. 19 LC8 alters the expression of Pin1 target proteins. T47D, PLC/PRF/5 and OVCAR3 cell lines were treated with 10 μM of ATRA (positive control) and 100 μM of LC8 for 24 hours and

analyzed by western blot. The expression of β-catenin, LC3B, and cyclin D1 was down regulated by LC8.

The growth promoting factors such as CyclinD1 and β-catenin were significant decreased after Pin1 inhibition, both in T47D, PLC/PRF/5 and OVCAR3 cells (Fig. 19).

How reported in literature, the chemical or genetic inhibition of Pin1 affect in strong manner the cyclin D1 protein, confirming that the liposomal formulation of Pin1 inhibitor (LC8) is specify for Pin1 and altered its function affecting also the direct targets. Interestingly, LC3B, an autophagy marker is also significantly changed.

The positive control ATRA provided similar results.

3.5 Maximum tolerated dose (MTD) of LC8

Liposomal drugs are mostly effective *in vivo* due to their designed formulation to accumulate inside the tumor (EPR effect) due also to the presence on the surface of PEG.

Before testing the efficacy of LC8, we carried out a maximum tolerated dose (MTD) experiments. Mice were treated with a dose escalation of the liposomal formulation (without drug) and the health of the mice was monitored. We found that the mice could be treated up to 250 $mgkg^{-1}$ of liposomes without evident signs of toxicity (Fig. 20 A,B).

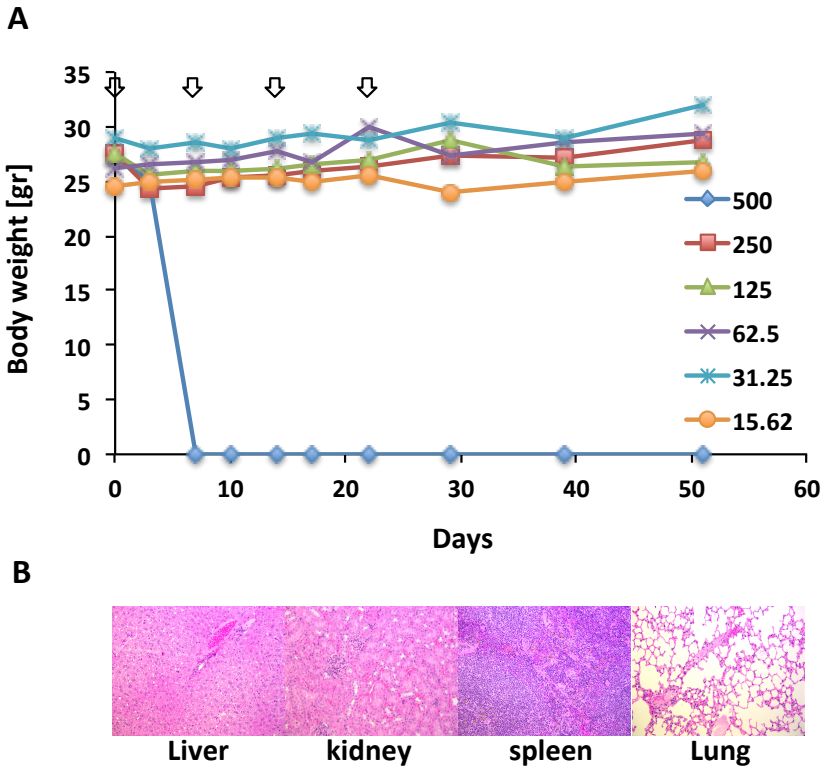

Fig.20 MTD analysis. FVB/N mice were i.p. injected every 7 days (arrows) at the indicated doses (mg/kg) of (A) empty liposomes. The mice treated with 250 mg/kg of empty liposomes were scarified and the tissues were H&E stained and analyzed with a 20X objective (B)

The weight of mice was monitored for almost 3 months, in order to follow the wellness of the mice. Then by hematoxylin and eosin staining it was defined and monitored if some toxic effect occurs at

tissue level. Here are reported only the tissues in which is know that a liposomal formulation can give toxic effect. No evidences of toxicity are observed.

Afterwards, the mice were treated i.p. with LC8 at the indicated doses. As an objective scale of mouse health, the body weight was followed for almost 3 months. We observed no sign of toxicity up to 40 $mgkg^{-1}$ (Fig. 20 C, D).

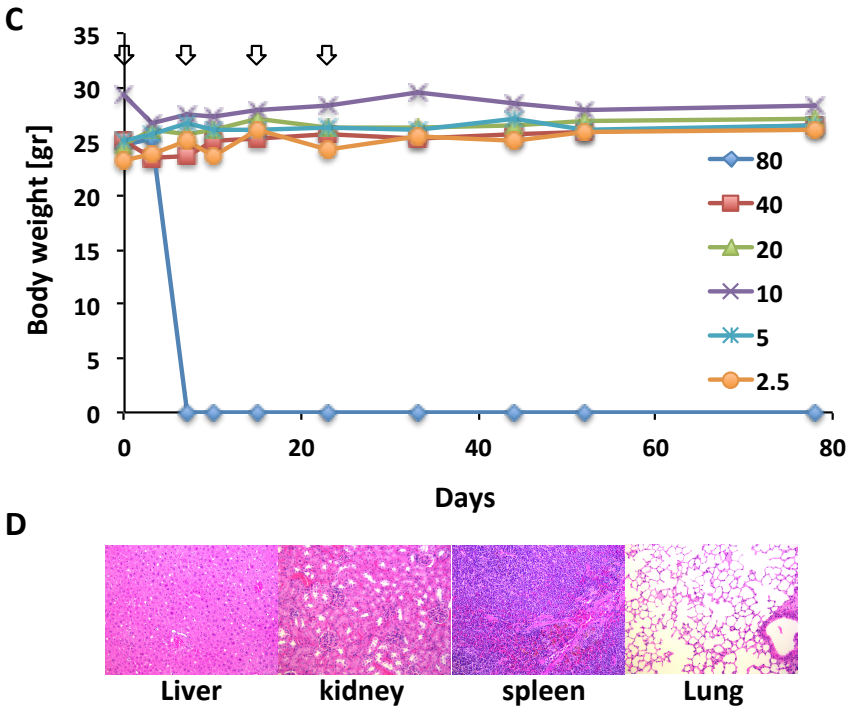

Fig.20 MTD analysis. FVB/N mice were i.p. injected every 7 days (arrows) at the indicated doses (mg/kg) of (C) LC8 and the body weight was recorded. The mice treated with 20 mg/kg of LC8 were scarified and the tissues were H&E stained and analyzed with a 20X objective (D).

3.6 LC8 is a drug for HGSOC therapy

OVCAR3 cells are a good model of HGSOC and can grow subcutaneously in nude mice. $5x10^6$ Cells were injected into the flank of the mice and after tumors reached a volume of 168.2 ± 27.97, the animals were treated with $20mgkg^{-1}$ of LC8 as in the MTD experiment. LC8 was injected i.p. every 7 days (arrows). LC8 significantly decreased tumor volume, compared to untreated mice (Fig. 21A), without compromising animal health. In fact, it was also monitored the body weight of the mice in both groups (Fig. 21B).

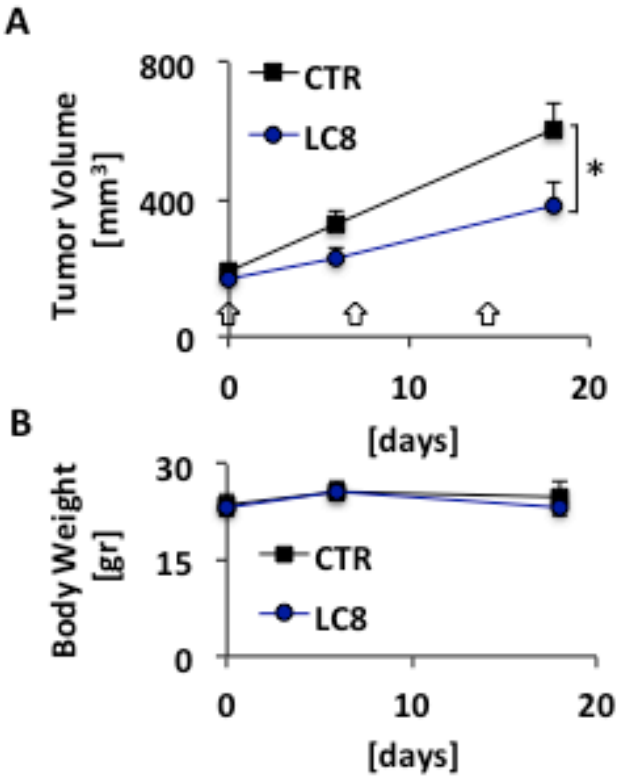

Fig. 21 LC8 is effective in a HGSOC mouse tumor model. Nude mice were subcutaneously injected with OVCAR3 cell line (n=12) and (A) tumor volume and (B) body weight were followed for 18 days.

Serum pharmacokinetic analysis of the drug showed two-kinetic phases of elimination, with a major decrement in the first 10h (Fig. 21C).

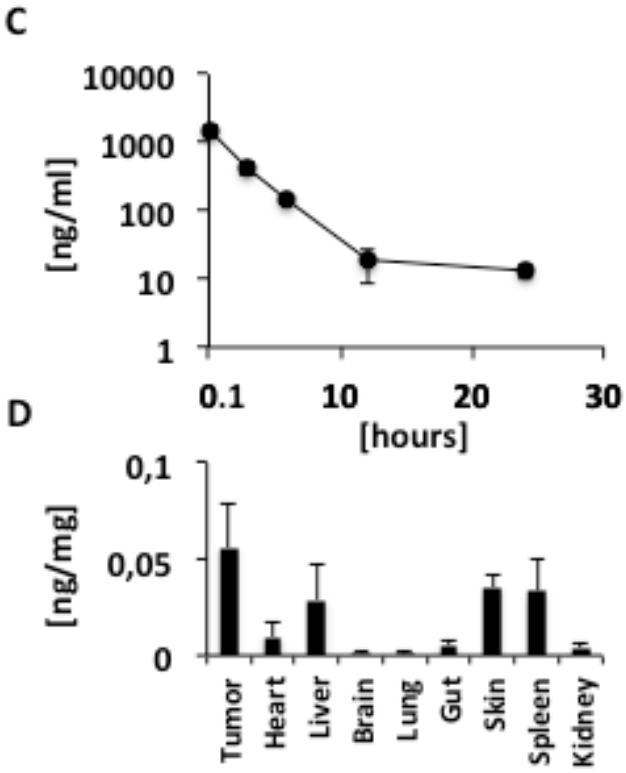

Fig. 21 LC8 is effective in a HGSOC mouse tumor model. (C) FVB/N mice (n=3, data point) were i.p. injected with 20 mg/kg and plasma was analyzed at indicated time point. (D) Nude mice (n=3, data point) subcutaneously implanted with OVCAR3 cell line were i.p. injected with 20 mg/kg of LC8 and analyzed after 72h. Y axis: ng of drug/mg of tissue.

Interestingly, the biodistribution of LC8 after 72h showed a main accumulation in the tumor followed by liver, spleen, and skin (Fig. 21 D).

Similar to Doxil[41], the liposomal formulation could avoid accumulation of doxorubicin in tissues with tight junctions and a well-developed lymphatic system such as heart. On the contrary, the tumor with a leaky vasculature and a poor lymphatic system allows the accumulation of LC8, in

turn increasing the efficacy of the drug. Although the circulation time of LC8 is far from Doxil, the volume of distribution is still low thus increasing the therapeutic index.

The effect of LC8 was evaluated on the expression of Pin1 in the tumors of mice treated with LC8 or untreated as in Fig. 21A and B. LC8 downregulated the expression of Pin1 at background level (negative) as showed in Fig. 21E. In untreated mice, Pin1 has an intense cytoplasmic/nuclear staining.

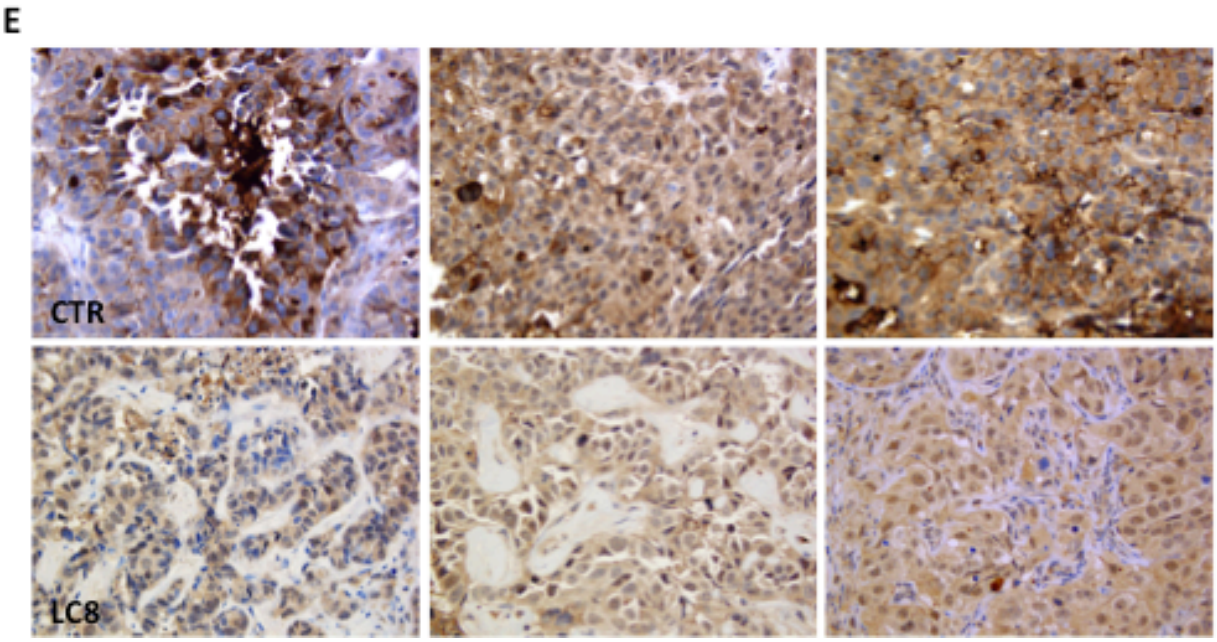

Fig. 21 LC8 is effective in a HGSOC mouse tumor model (E) IHC evaluation of Pin1 expression in 3 tumors derived from (A and B).

4. Discussions and conclusions

Ovarian cancer is one of the most serious diseases worldwide and the fifth-most common cancer among women. The prolyl-isomerase PIN1 represents a critical player in several oncogenic signalling, and as consequence of this function, PIN1 inhibition causes the collapse of numerous oncogenic pathways. The central role of Pin1 making it an attractive drug target for the development of treatments against cancer. The available PIN1 inhibitors either lack the required specificity and/or potency, or cannot efficiently enter cells to inhibit PIN1 function *in vivo*. Several PIN1 inhibitors have been identified with both covalent and non-covalent mechanisms of action. Juglone covalently interacts with PIN1 catalytic domain but presents several off-targets so it is no so specify for PIN1. Recently ATRA has been shown activity in cells and in mouse models and the inhibitor developed by De Sal, KPT-6566, binds covalently the Pin1 protein. This type of binding is no desirable: it is better to have an inhibitor that reversible interacts and binds its target.

Recently, it was demonstrated that Pin1 is also able to regulate the biogenesis of miRNA, which is aberrantly expressed in HCC and promotes HCC progression. The authors of this investigation reported that a new Pin1 inhibitor, AF-39, is able to inhibit Pin1 activity and suppresses cell proliferation of HCC cells in a dose- and time-dependent manner [98]. AF‐39 regulates the subcellular distribution of XPO5 and increases miRNAs biogenesis in HCC cells. The authors did not report the *in vivo* activity.

Another inhibitor, already reported in the literature, Celasterol,extracted from Thunder God Vine, was studied in order to define its activity on different ovarian cancer cells. The authors reported the anti-cancer efficacy of this compound and the G2/M cell cycle arrest after the treatments. This compound is also able to down-regulate different PIN1 substrates and to induce the apoptosis. No *in vivo* studies were reported [99].

In this investigation was defining the crucial role of Pin1 in ovarian cancer. When Pin1 is down regulated in human serous ovarian cancer cell line (STOSE), the cells lose the capability to form tumors in a mouse model.

This study also reports the preparation of an effective liposomal formulation of a potent and selective Pin1 inhibitor. For the first time, it was encapsulated a selective Pin1 inhibitor, designed by Pfizer, into liposomes [68]. Utilizing a similar method developed by Vogelstein's group [90], successfully the drug/modified cyclodextrin complex was loaded by remote loading into liposomes and utilized to kill ovarian cancer cells not only *in vitro* but also in an *in vivo* model. The new nanoformulation dramatically improves the *in vitro* and in *vivo* pharmacological properties of the Pin1 inhibitor. The inhibitor developed by Pfizer is very specific for PIN1 but it is enable to enter inside the cells. It was consistently observed that the liposomal formulation retains the inhibitor and also permits it to enter inside the cells.

It was observed that LC8 treatment of NIH 3T3 cells caused a decrease of endogenous PIN1 levels in dose and time dependent manner, and promoted the PIN1 proteasomal degradation. Notably, the LC8 formulation not only kill the ovarian cancer cells but also is able to down regulate the expression of PIN1 and its mainly targets (Cyclin D, β-Catenin and LC3B).

Finally, the liposomal formulation is able to reduce the tumor volume when injected in mice and down regulate the expression of Pin1 *in vivo*, without any toxic effects. It is interesting that the IHC of the tumors of mice treated with LC8 reveals down regulation of Pin1 at background level.

In summary, we showed that LC8 directly binds, inhibits and degrades the active form of Pin1 that is overexpressed in many cancer cells to exert potent anticancer, probably by blocking multiple cancer-driving pathways at once. Our findings offer a promising new approach to stop numerous cancer-driving molecules and inhibit cancer cells. The development of such new active liposome formulations may pave the way for clinical experimentation and support for a new effective targeted therapy for ovarian cancer patients.

BIBLIOGRAPY

1. Luvero, D., Milani, A. & Ledermann, J. A. Treatment options in recurrent ovarian cancer: latest evidence and clinical potential. *Ther. Adv. Med. Oncol.* **6,** 229–239 (2014).
2. Romero, I., Bast, R. C. & Jr. Minireview: human ovarian cancer: biology, current management, and paths to personalizing therapy. *Endocrinology* **153,** 1593–602 (2012).
3. Vaughan, S. *et al.* Rethinking ovarian cancer: Recommendations for improving outcomes. *Nature Reviews Cancer* (2011).
4. Kim, J. *et al.* High-grade serous ovarian cancer arises from fallopian tube in a mouse model. *Proc. Natl. Acad. Sci.* **109,** 3921–3926 (2012).
5. van Dorp, W. *et al.* Reproductive Function and Outcomes in Female Survivors of Childhood, Adolescent, and Young Adult Cancer: A Review. *J. Clin. Oncol.* JCO.2017.76.344 (2018).
6. Mutch, D. G. Surgical management of ovarian cancer. *Semin. Oncol.* **29,** 3–8 (2002).
7. Ledermann, J. A. *et al.* Newly diagnosed and relapsed epithelial ovarian carcinoma: ESMO Clinical Practice Guidelines for diagnosis, treatment and follow-up. *Ann. Oncol.* **29,** iv259-iv259 (2018).
8. Morgan, R. J. *et al.* Ovarian cancer, version 3.2012. *J. Natl. Compr. Canc. Netw.* **10,** 1339–49 (2012).
9. Lambert, H. E. & Berry, R. J. High dose cisplatin compared with high dose cyclophosphamide in the management of advanced epithelial ovarian cancer (FIGO stages III and IV): report from the North Thames Cooperative Group. *Br. Med. J. (Clin. Res. Ed).* **290,** 889–93 (1985).
10. Piccart, M. J. *et al.* Randomized intergroup trial of cisplatin-paclitaxel versus cisplatin-cyclophosphamide in women with advanced epithelial ovarian cancer: three-year results. *J. Natl. Cancer Inst.* **92,** 699–708 (2000).
11. McGuire, W. P. *et al.* Comparison of combination therapy with paclitaxel and cisplatin

versus cyclophosphamide and cisplatin in patients with suboptimal stage III and stage IV ovarian cancer: a Gynecologic Oncology Group study. *Semin. Oncol.* **24,** S2-13-S2-16 (1997).

12. Pepa, C. Della *et al.* Ovarian cancer standard of care: are there real alternatives? *Chin. J. Cancer* **34,** 17–27 (2015).
13. Zhang, H. *et al.* Integrated Proteogenomic Characterization of Human High-Grade Serous Ovarian Cancer. *Cell* **166,** 755–765 (2016).
14. Bell, D. *et al.* Integrated genomic analyses of ovarian carcinoma. *Nature* **474,** 609–615 (2011).
15. Girardini, J. E. *et al.* A Pin1/mutant p53 axis promotes aggressiveness in breast cancer. *Cancer Cell* **20,** 79–91 (2011).
16. Zhou, X. Z. & Lu, K. P. The isomerase PIN1 controls numerous cancer-driving pathways and is a unique drug target. *Nat. Rev. Cancer* **16,** 463–478 (2016).
17. Zhou, X. Z. *et al.* Pin1-Dependent Prolyl Isomerization Regulates Dephosphorylation of Cdc25C and Tau Proteins. *Mol. Cell* **6,** 873–883 (2000).
18. Peng, T., Zintsmaster, J. S., Namanja, A. T. & Peng, J. W. Sequence-specific dynamics modulate recognition specificity in WW domains. *Nat. Struct. Mol. Biol.* **14,** 325–331 (2007).
19. Shaw, P. E. Peptidyl-prolyl cis/trans isomerases and transcription: is there a twist in the tail? *EMBO Rep.* **8,** 40–45 (2007).
20. Balastik, M., Lim, J., Pastorino, L. & Lu, K. P. Pin1 in Alzheimer's disease: Multiple substrates, one regulatory mechanism? *Biochim. Biophys. Acta - Mol. Basis Dis.* **1772,** 422–429 (2007).
21. Ping Lu, K., Hanes, S. D. & Hunter, T. A human peptidyl–prolyl isomerase essential for regulation of mitosis. *Nature* **380,** 544–547 (1996).
22. Ranganathan, R., Lu, K. P., Hunter, T. & Noel, J. P. Structural and functional analysis of the

mitotic rotamase Pin1 suggests substrate recognition is phosphorylation dependent. *Cell* **89,** 875–86 (1997).

23. Lu, P. J., Zhou, X. Z., Shen, M. & Lu, K. P. Function of WW domains as phosphoserine- or phosphothreonine-binding modules. *Science* **283,** 1325–8 (1999).

24. Ryo, A., Nakamura, M., Wulf, G., Liou, Y.-C. & Lu, K. P. Pin1 regulates turnover and subcellular localization of β-catenin by inhibiting its interaction with APC. *Nat. Cell Biol.* **3,** 793–801 (2001).

25. Wulf, G. M. Pin1 is overexpressed in breast cancer and cooperates with Ras signaling in increasing the transcriptional activity of c-Jun towards cyclin D1. *EMBO J.* **20,** 3459–3472 (2001).

26. Lu, K. P. & Zhou, X. Z. The prolyl isomerase PIN1: a pivotal new twist in phosphorylation signalling and disease. *Nat Rev Mol Cell Biol* **8,** 904–916 (2007).

27. Verdecia, M. A., Bowman, M. E., Lu, K. P., Hunter, T. & Noel, J. P. Structural basis for phosphoserine-proline recognition by group IV WW domains. *Nat. Struct. Biol.* **7,** 639–43 (2000).

28. Wintjens, R. *et al.* ^{1}H NMR Study on the Binding of Pin1 Trp-Trp Domain with Phosphothreonine Peptides. *J. Biol. Chem.* **276,** 25150–25156 (2001).

29. Lu, P.-J., Zhou, X. Z., Liou, Y.-C., Noel, J. P. & Lu, K. P. Critical Role of WW Domain Phosphorylation in Regulating Phosphoserine Binding Activity and Pin1 Function. *J. Biol. Chem.* **277,** 2381–2384 (2002).

30. Ryo, A. *et al.* Regulation of NF-kappaB signaling by Pin1-dependent prolyl isomerization and ubiquitin-mediated proteolysis of p65/RelA. *Mol. Cell* **12,** 1413–26 (2003).

31. Zacchi, P. *et al.* The prolyl isomerase Pin1 reveals a mechanism to control p53 functions after genotoxic insults. *Nature* **419,** 853–7 (2002).

32. Girardini, J. E. *et al.* A Pin1/mutant p53 axis promotes aggressiveness in breast cancer. *Cancer Cell* **20,** 79–91 (2011).

33. Wulf, G. M. *et al.* Pin1 is overexpressed in breast cancer and cooperates with Ras signaling in increasing the transcriptional activity of c-Jun towards cyclin D1. *EMBO J.* **20,** 3459–72 (2001).

34. Bao, L. *et al.* Prevalent Overexpression of Prolyl Isomerase Pin1 in Human Cancers. *Am. J. Pathol.* **164,** 1727–1737 (2004).

35. Blume-Jensen, P. & Hunter, T. Oncogenic kinase signalling. *Nature* **411,** 355–365 (2001).

36. Lu, K. P. Prolyl isomerase Pin1 as a molecular target for cancer diagnostics and therapeutics. *Cancer Cell* **4,** 175–80 (2003).

37. Lu, K. P. *et al.* Targeting carcinogenesis: A role for the prolyl isomerase Pin1? *Mol. Carcinog.* **45,** 397–402 (2006).

38. Cheng, C.-W. *et al.* PIN1 Inhibits Apoptosis in Hepatocellular Carcinoma through Modulation of the Antiapoptotic Function of Survivin. *Am. J. Pathol.* **182,** 765–775 (2013).

39. Pang, R. *et al.* Pin1 interacts with a specific serine-proline motif of hepatitis B virus X-protein to enhance hepatocarcinogenesis. *Gastroenterology* **132,** 1088–103 (2007).

40. Pang, R. W. *et al.* PIN1 expression contributes to hepatic carcinogenesis. *J. Pathol.* **210,** 19–25 (2006).

41. Suizu, F., Ryo, A., Wulf, G., Lim, J. & Lu, K. P. Pin1 regulates centrosome duplication, and its overexpression induces centrosome amplification, chromosome instability, and oncogenesis. *Mol. Cell. Biol.* **26,** 1463–79 (2006).

42. Ayala, G. *et al.* The prolyl isomerase Pin1 is a novel prognostic marker in human prostate cancer. *Cancer Res.* **63,** 6244–51 (2003).

43. Bao, L. *et al.* Prevalent overexpression of prolyl isomerase Pin1 in human cancers. *Am J Pathol* **164,** 1727–1737 (2004).

44. Pang, R. *et al.* PIN1 overexpression and beta-catenin gene mutations are distinct oncogenic events in human hepatocellular carcinoma. *Oncogene* **23,** 4182–6 (2004).

45. Ryo, A. *et al.* Stable suppression of tumorigenicity by Pin1-targeted RNA interference in

prostate cancer. *Clin. Cancer Res.* **11,** 7523–31 (2005).

46. Ryo, A. *et al.* PIN1 Is an E2F Target Gene Essential for Neu/Ras-Induced Transformation of Mammary Epithelial Cells. *Mol. Cell. Biol.* **22,** 5281–5295 (2002).

47. Gianni, M. *et al.* Inhibition of the peptidyl-prolyl-isomerase Pin1 enhances the responses of acute myeloid leukemia cells to retinoic acid via stabilization of RARalpha and PML-RARalpha. *Cancer Res* **69,** 1016–1026 (2009).

48. Girardini, J. E. *et al.* A Pin1/mutant p53 axis promotes aggressiveness in breast cancer. *Cancer Cell* **20,** 79–91 (2011).

49. La Montagna, R. *et al.* Androgen receptor serine 81 mediates Pin1 interaction and activity. *Cell Cycle* **11,** 3415–20 (2012).

50. Rizzolio, F. *et al.* Retinoblastoma tumor-suppressor protein phosphorylation and inactivation depend on direct interaction with Pin1. *Cell Death Differ.* **19,** 1152–1161 (2012).

51. Lucchetti, C., Caligiuri, I., Toffoli, G., Giordano, A. & Rizzolio, F. The prolyl isomerase Pin1 acts synergistically with CDK2 to regulate the basal activity of estrogen receptor α in breast cancer. *PLoS One* **8,** e55355 (2013).

52. La Montagna, R., Caligiuri, I., Giordano, A. & Rizzolio, F. Pin1 and nuclear receptors: A new language? *J. Cell. Physiol.* **228,** 1799–801 (2013).

53. Rizzolio, F. *et al.* Dissecting Pin1 and phospho-pRb regulation. *J. Cell. Physiol.* **228,** 73–77 (2013).

54. Moore, J. D. & Potter, A. Pin1 inhibitors: Pitfalls, progress and cellular pharmacology. *Bioorg. Med. Chem. Lett.* **23,** 4283–4291 (2013).

55. Liou, Y. C. *et al.* Loss of Pin1 function in the mouse causes phenotypes resembling cyclin D1-null phenotypes. *Proc Natl Acad Sci U S A* **99,** 1335–1340 (2002).

56. Lu, Z. & Hunter, T. Prolyl isomerase Pin1 in cancer. *Cell Res.* **24,** 1033–1049 (2014).

57. Singh, A. & Settleman, J. EMT, cancer stem cells and drug resistance: an emerging axis of evil in the war on cancer. *Oncogene* **29,** 4741–4751 (2010).

58. Rustighi, A. *et al.* Prolyl-isomerase Pin1 controls normal and cancer stem cells of the breast. *EMBO Mol. Med.* **6,** 99–119 (2014).

59. Ding, Q. *et al.* Down-regulation of Myeloid Cell Leukemia-1 through Inhibiting Erk/Pin 1 Pathway by Sorafenib Facilitates Chemosensitization in Breast Cancer. *Cancer Res.* **68,** 6109–6117 (2008).

60. Wang, J., Liu, K., Wang, X.-F. & Sun, D.-J. Juglone reduces growth and migration of U251 glioblastoma cells and disrupts angiogenesis. *Oncol. Rep.* **38,** 1959–1966 (2017).

61. Kanaoka, R. *et al.* Pin1 Inhibitor Juglone Exerts Anti-Oncogenic Effects on LNCaP and DU145 Cells despite the Patterns of Gene Regulation by Pin1 Differing between These Cell Lines. *PLoS One* **10,** e0127467 (2015).

62. Lee, N. Y. *et al.* The prolyl isomerase Pin1 interacts with a ribosomal protein S6 kinase to enhance insulin-induced AP-1 activity and cellular transformation. *Carcinogenesis* **30,** 671–681 (2009).

63. Hennig, L. *et al.* Selective inactivation of parvulin-like peptidyl-prolyl cis/trans isomerases by juglone. *Biochemistry* **37,** 5953–60 (1998).

64. Tatara, Y., Lin, Y.-C., Bamba, Y., Mori, T. & Uchida, T. Dipentamethylene thiuram monosulfide is a novel inhibitor of Pin1. *Biochem. Biophys. Res. Commun.* **384,** 394–8 (2009).

65. Uchida, T. *et al.* Pin1 and Par14 peptidyl prolyl isomerase inhibitors block cell proliferation. *Chem. Biol.* **10,** 15–24 (2003).

66. Guo, C. *et al.* Structure-based design of novel human Pin1 inhibitors (I). *Bioorg. Med. Chem. Lett.* **19,** 5613–6 (2009).

67. Dong, L. *et al.* Structure-based design of novel human Pin1 inhibitors (II). *Bioorg. Med. Chem. Lett.* **20,** 2210–2214 (2010).

68. Guo, C. *et al.* Structure-based design of novel human Pin1 inhibitors (III): Optimizing affinity beyond the phosphate recognition pocket. *Bioorg. Med. Chem. Lett.* **24,** 4187–4191

(2014).

69. Potter, A. J. *et al.* Structure-guided design of alpha-amino acid-derived Pin1 inhibitors. *Bioorg. Med. Chem. Lett.* **20,** 586–90 (2010).

70. Liao, X.-H. *et al.* Chemical or genetic Pin1 inhibition exerts potent anticancer activity against hepatocellular carcinoma by blocking multiple cancer-driving pathways. *Sci. Rep.* **7,** 43639 (2017).

71. Wei, S. *et al.* Active Pin1 is a key target of all-trans retinoic acid in acute promyelocytic leukemia and breast cancer. *Nat. Med.* **21,** 457–66 (2015).

72. Campaner, E. *et al.* A covalent PIN1 inhibitor selectively targets cancer cells by a dual mechanism of action. *Nat. Commun.* **8,** 15772 (2017).

73. A J Sinclair G Peters, and P J Farrell, I. P. EBNA-2 and EBNA-LP cooperate to cause G0 to G1 transition during immortalization of resting human B lymphocytes by Epstein-Barr virus. *EMBO J* **13,** (1994).

74. Blanco, E., Shen, H. & Ferrari, M. Principles of nanoparticle design for overcoming biological barriers to drug delivery. *Nat. Biotechnol.* **33,** 941–951 (2015).

75. Matsumura, Y. & Maeda, H. A new concept for macromolecular therapeutics in cancer chemotherapy: mechanism of tumoritropic accumulation of proteins and the antitumor agent smancs. *Cancer Res.* **46,** 6387–92 (1986).

76. Aggarwal, P., Hall, J. B., McLeland, C. B., Dobrovolskaia, M. A. & McNeil, S. E. Nanoparticle interaction with plasma proteins as it relates to particle biodistribution, biocompatibility and therapeutic efficacy. *Adv. Drug Deliv. Rev.* **61,** 428–437 (2009).

77. Wang, A. Z., Langer, R. & Farokhzad, O. C. Nanoparticle Delivery of Cancer Drugs. *Annu. Rev. Med.* **63,** 185–198 (2012).

78. Farokhzad, O. C. & Langer, R. Impact of Nanotechnology on Drug Delivery. (2009).

79. Barenholz, Y. Doxil®--the first FDA-approved nano-drug: lessons learned. *J. Control. Release* **160,** 117–34 (2012).

80. Miele, E., Spinelli, G. P., Miele, E., Tomao, F. & Tomao, S. Albumin-bound formulation of paclitaxel (Abraxane ABI-007) in the treatment of breast cancer. *Int. J. Nanomedicine* **4,** 99–105 (2009).

81. Torchilin, V. P. Recent advances with liposomes as pharmaceutical carriers. *Nat. Rev. Drug Discov.* **4,** 145–160 (2005).

82. Jesorka, A. & Orwar, O. Liposomes: Technologies and Analytical Applications. *Annu. Rev. Anal. Chem.* **1,** 801–832 (2008).

83. Parhi, R. & Suresh, P. Preparation and characterization of solid lipid nanoparticles-a review. *Curr. Drug Discov. Technol.* **9,** 2–16 (2012).

84. Un, K., Sakai-Kato, K., Oshima, Y., Kawanishi, T. & Okuda, H. Intracellular trafficking mechanism, from intracellular uptake to extracellular efflux, for phospholipid/cholesterol liposomes. *Biomaterials* **33,** 8131–8141 (2012).

85. Immordino, M. L., Dosio, F. & Cattel, L. Stealth liposomes: review of the basic science, rationale, and clinical applications, existing and potential. *Int. J. Nanomedicine* **1,** 297–315 (2006).

86. Park, J. W. Liposome-based drug delivery in breast cancer treatment. *Breast Cancer Res.* **4,** 95–9 (2002).

87. Bangham, A. D., Standish, M. M. & Watkins, J. C. Diffusion of univalent ions across the lamellae of swollen phospholipids. *J. Mol. Biol.* **13,** 238–52 (1965).

88. Mross, K. *et al.* Pharmacokinetics of liposomal doxorubicin (TLC-D99; Myocet) in patients with solid tumors: an open-label, single-dose study. *Cancer Chemother. Pharmacol.* **54,** 514–24 (2004).

89. Dong, L. *et al.* Structure-based design of novel human Pin1 inhibitors (II). *Bioorg. Med. Chem. Lett.* **20,** 2210–4 (2010).

90. Sur, S., Fries, A. C., Kinzler, K. W., Zhou, S. & Vogelstein, B. Remote loading of preencapsulated drugs into stealth liposomes. *Proc. Natl. Acad. Sci.* **111,** 2283–2288 (2014).

91. Russo Spena, C. *et al.* Liposomal delivery of a Pin1 inhibitor complexed with cyclodextrins as new therapy for high-grade serous ovarian cancer. *J. Control. Release* **281,** 1–10 (2018).

92. McCloskey, C. W. *et al.* A new spontaneously transformed syngeneic model of high-grade serous ovarian cancer with a tumor-initiating cell population. *Front. Oncol.* **4,** 53 (2014).

93. Chang, H.-I. & Yeh, M.-K. Clinical development of liposome-based drugs: formulation, characterization, and therapeutic efficacy. *Int. J. Nanomedicine* **7,** 49–60 (2012).

94. Gabizon, A., Shmeeda, H. & Barenholz, Y. Pharmacokinetics of pegylated liposomal Doxorubicin: review of animal and human studies. *Clin. Pharmacokinet.* **42,** 419–36 (2003).

95. Gubernator, J. Active methods of drug loading into liposomes: recent strategies for stable drug entrapment and increased *in vivo* activity. *Expert Opin. Drug Deliv.* **8,** 565–580 (2011).

96. Liao, X.-H. *et al.* Chemical or genetic Pin1 inhibition exerts potent anticancer activity against hepatocellular carcinoma by blocking multiple cancer-driving pathways. *Sci. Rep.* **7,** 43639 (2017).

97. Campaner, E. *et al.* A covalent PIN1 inhibitor selectively targets cancer cells by a dual mechanism of action. *Nat. Commun.* **8,** 15772 (2017).

98. Pu, W. *et al.* Targeting Pin1 by inhibitor API-1 regulates microRNA biogenesis and suppresses hepatocellular carcinoma development. *Hepatology* **68,** 547–560 (2018).

99. Li, X. *et al.* Celastrol strongly inhibits proliferation, migration and cancer stem cell properties through suppression of Pin1 in ovarian cancer cells. *Eur. J. Pharmacol.* **842,** 146–156 (2019).

Acknowledgments

I would like to express my sincere gratitude to my supervisor Prof. Grassi and co-supervisor Dott. Rizzolio. Also, I would like to thank Barbara and Lucia, Stefano, Mommy, Maggy and Nayla.

Last but not the least, I would like to thank my family for supporting me.